






# Akkermansia muciniphila induces slow extramedullary hematopoiesis via cooperative IL-1R/TLR signals

Yuxin Wang<sup>1,2</sup> , Tatsuya Morishima<sup>2,3</sup> , Maiko Sezaki<sup>2,3</sup>, Ryo Sato<sup>2</sup>, Gaku Nakato<sup>4</sup>, Shinji Fukuda<sup>4,5,6</sup> , Kouji Kobiyama<sup>7,8</sup>, Ken J Ishii<sup>7,8</sup> , Yuhua Li<sup>1,9,\*\*,†</sup> & Hitoshi Takizawa<sup>2,10,\*</sup> 

## Abstract

Bacterial infections can activate and mobilize hematopoietic stem and progenitor cells (HSPCs) from the bone marrow (BM) to the spleen, a process termed extramedullary hematopoiesis (EMH). Recent studies suggest that commensal bacteria regulate not only the host immune system but also hematopoietic homeostasis. However, the impact of gut microbes on hematopoietic pathology remains unclear. Here, we find that systemic single injections of *Akkermansia muciniphila* (*A. m.*), a mucin-degrading bacterium, rapidly activate BM myelopoiesis and slow but long-lasting hepato-splenomegaly, characterized by the expansion and differentiation of functional HSPCs, which we term delayed EMH. Mechanistically, delayed EMH triggered by *A. m.* is mediated entirely by the MYD88/TRIF innate immune signaling pathway, which persistently stimulates splenic myeloid cells to secrete interleukin (IL)-1 $\alpha$ , and in turn, activates IL-1 receptor (IL-1R)-expressing splenic HSPCs. Genetic deletion of Toll-like receptor-2 and -4 (TLR2/4) or IL-1 $\alpha$  partially diminishes *A. m.*-induced delayed EMH, while inhibition of both pathways alleviates splenomegaly and EMH. Our results demonstrate that cooperative IL-1R- and TLR-mediated signals regulate commensal bacteria-driven EMH, which might be relevant for certain autoimmune disorders.

**Keywords** *Akkermansia muciniphila*; extramedullary hematopoiesis; hematopoietic stem and progenitor cell; IL-1; TLR

**Subject Categories** Microbiology, Virology & Host Pathogen Interaction; Signal Transduction; Stem Cells & Regenerative Medicine

**DOI** 10.15252/embr.202357485 | Received 14 May 2023 | Revised 3 October 2023 | Accepted 6 October 2023 | Published online 23 October 2023

**EMBO Reports (2023) 24: e57485**

## Introduction

Commensal microbes coexist within the human body and reach a cell number more than total human cells (Sender *et al.*, 2016), ca.  $4 \times 10^{13}$ , and have been recently shown to significantly affect the maintenance and activation of the immune system (Biragyn & Ferrucci, 2018; Ruff *et al.*, 2020). Among them, the microbiota colonized in the gut has been shown to regulate hematopoietic development (Lee *et al.*, 2019), steady-state hematopoiesis (Balmer *et al.*, 2014; Khosravi *et al.*, 2014), and hematopoietic stem cell (HSC) aging (Kovtonyuk *et al.*, 2021). *Akkermansia muciniphila* (*A. m.*) is an anaerobic gram-negative bacterium and one of the major mucin-associated microbial species found in the human gut, which accounts for 1–5% of the entire microbial community (Derrien *et al.*, 2008). They reside in the mucus layer as a mucin-degrading bacterium (Derrien *et al.*, 2004), and their increase can alleviate metabolic syndromes (Plovier *et al.*, 2017), inflammatory bowel diseases (IBD; Wu *et al.*, 2021), and PD-1-based immunotherapy against epithelial cancer (Routy *et al.*, 2018) as well as non-small-cell lung cancer (Derosa *et al.*, 2022). In contrast to these beneficial roles, *A. m.* has been associated with increased intestinal inflammation (Ganesh *et al.*, 2013) and increased GVHD-related mortality (Shono *et al.*, 2016) through activating the immune system when translocated into peritoneal cavity, suggesting their additional pathological roles in immune system control. In addition, our previous study has also observed a significant increase of *A. m.* after colitis induction in a mouse model (Sezaki *et al.*, 2020). Yet, how *A. m.* affects the hematopoietic system and its pathogenesis has not been reported.

In the steady state, adult HSCs are homeostatically maintained in the bone marrow (BM), where specific niche cells support HSC

1 Department of Hematology, Zhujiang Hospital, Southern Medical University, Guangzhou, China

2 Laboratory of Stem Cell Stress, International Research Center for Medical Sciences (IRCMS), Kumamoto University, Kumamoto, Japan

3 Laboratory of Hematopoietic Stem Cell Engineering, IRCMS, Kumamoto University, Kumamoto, Japan

4 Gut Environmental Design Group, Kanagawa Institute of Industrial Science and Technology, Atsugi, Japan

5 Institute for Advanced Biosciences (IAB), Keio University, Tokyo, Japan

6 Transborder Medical Research Center, University of Tsukuba, Tsukuba, Japan

7 Division of Vaccine Science, Department of Microbiology and Immunology, The Institute of Medical Science, The University of Tokyo, Tokyo, Japan

8 International Vaccine Design Center, The Institute of Medical Science, The University of Tokyo, Tokyo, Japan

9 Bioland Laboratory (Guangzhou Regenerative Medicine and Health Guangdong Laboratory), Guangzhou, China

10 Center for Metabolic Regulation of Healthy Aging (CMHA), Kumamoto University, Kumamoto, Japan

\*Corresponding author. Tel: +81 96 373 6879; E-mail: [htakizawa@kumamoto-u.ac.jp](mailto:htakizawa@kumamoto-u.ac.jp)

\*\*Corresponding author. Tel: +86 020 62782316; E-mail: [liyuhua1974@outlook.com](mailto:liyuhua1974@outlook.com)

†Correction added on 6 December 2023, after first online publication: Yuhua Li has been corrected from co-senior author to co-corresponding author.

maintenance and quiescence, while only a very minor population of HSCs can be found in other organs such as the peripheral blood (PB; Wright *et al*, 2001), lymph duct (Massberg *et al*, 2007), spleen (Morita *et al*, 2011), and gingiva (Krishnan *et al*, 2021). In contrast, under hematopoietic stress conditions such as infection (Burberry *et al*, 2014) or chemotherapy (Inra *et al*, 2015), HSCs are activated and mobilized from the BM to other organs such as the spleen and liver to enhance hematopoiesis and replenish cell types that are in high demand, which is called extramedullary hematopoiesis (EMH). EMH is known to be mediated by cytokine/chemokine receptors that sense the inflammatory milieu released from proximal/distal organs, including granulocyte colony-stimulating factor receptor (G-CSFR; Burberry *et al*, 2014), c-Kit, CXCR4 (Inra *et al*, 2015), and pattern recognition receptors (PRRs) such as Toll-like receptors (TLRs), NOD-like receptors (NLRs; Burberry *et al*, 2014) and C-type lectin receptors (CLRs; Nakamura-Ishizu *et al*, 2015).

In addition to PRRs, another innate immune sensor is the interleukin (IL)-1 receptor, which binds to IL-1 $\alpha$  or IL-1 $\beta$ , and triggers its downstream transcriptional responses via the adaptor protein MyD88 (Sims & Smith, 2010). While IL-1 $\beta$  is secreted systemically and circulates throughout different tissues, IL-1 $\alpha$  is produced locally in inflamed tissues by various hematopoietic (e.g., monocytes; Chan *et al*, 2015), granulocytes, and dendritic cells (Mayer-Barber *et al*, 2011) and non-hematopoietic cells. IL-1 $\alpha$  is crucial for sustaining inflammatory responses (Lukens *et al*, 2013), recruiting myeloid cells to infected tissues (Di Paolo & Shayakhmetov, 2016), hematopoietic stem and progenitor cell (HSPC) mobilization, and expansion (Neta *et al*, 1987; Fibbe *et al*, 1992).

In this study, we found for the first time that (i) single administration of the *A. m.* membrane fraction induces drastic, long-lasting anemia and hepato-splenomegaly with immune cell and HSPC activation, (ii) there are two temporal waves of HSPC expansion causing EMH upon *A. m.* injection, the latter with functional HSPCs accumulated in the spleen, (iii) *A. m.*-induced EMH is mediated entirely by MYD88/TRIF-dependent innate immune signals, and partially by TLR2/4- and IL-1 $\alpha$ -dependent signals, (iv) sustained secretion of IL-1 $\alpha$  from splenic myeloid cells activate IL-1R-expressing splenic HSPCs, and (v) pharmacological inhibition of IL-1R in addition to TLR2/4 genetic ablation completely alleviates EMH. These findings shed light into the pathophysiology of *A. m.*-

associated metabolic and inflammatory disorders, and IL-1-related chronic hemato-immune disorders such as stem cell aging, clonal hematopoiesis, and autoimmune diseases.

## Results

### A single injection of live *A. m.* or its membrane fraction induces long-lasting anemia and hepatosplenomegaly with extramedullary hematopoiesis

To study the impact of *A. m.* on the hematopoietic system, either live *A. m.* ( $10^7$ – $10^9$  CFU) or the *A. m.* membrane fraction, 200  $\mu$ g (equivalent to  $10^8$  CFU) were *i.p.* injected into wild-type (WT) mice. Both live *A. m.* and its lysate induced severe splenomegaly (Fig 1A and B, and Appendix Fig S1A), which was not reproducible by injection of lysate derived from another gram-negative commensal bacterium, *Bacteroides thetaiotaomicron* (*B. t.*; Fig 1C and D). This suggests that *A. m.*-specific membrane component has a potential to induce splenomegaly. Thus, we decided to use 200  $\mu$ g of lysate for the rest of all experiments. PB counts of *A. m.*-injected mice showed pancytopenia with a sudden decrease in white blood cell (WBC) and platelet (PLT) counts on day 1 post-injection (Appendix Fig S1B). Intriguingly, *A. m.*-treated mice showed sustained severe anemia and hepato-splenomegaly (Pearson correlation coefficient for spleen and liver size: 0.714), which peaked at day 14 and lasted for almost 2 months after a single injection (Appendix Fig S1C–E). The total cell number of splenocytes followed the same kinetics (Fig 1E).

To dissect which cells expanded in *A. m.*-treated spleen, mature and immature hematopoietic cell fractions were immunophenotyped at day 14 post-injection (Fig 1F–I and Appendix Fig S1F–H). Percentage of myeloid cells such as neutrophils (CD11b<sup>+</sup>Ly6G<sup>+</sup>), eosinophils (CD11b<sup>+</sup>Ly6G<sup>-</sup>F4/80<sup>+</sup>SSC-H<sup>high</sup>) and Ly-6C<sup>+</sup> monocytes (CD11b<sup>+</sup>Ly6G<sup>-</sup>F4/80<sup>+</sup>SSC-H<sup>low</sup>Ly-6C<sup>+</sup>) expanded significantly in *A. m.*-injected spleen compared to PBS controls, whereas the percentage of B and T cells decreased (Fig 1F and G). The population with the most significant increase was CD3 $\epsilon$ <sup>-</sup>B220<sup>-</sup>CD11b<sup>-</sup>CD11<sup>-</sup> (blue gate), containing both non-hematopoietic cells and immature HSPCs (Fig 1H), with a fold expansion of 8.5 ( $4.72 \pm 1.71\%$  in

**Figure 1. A single *Akkermansia muciniphila* injection induces long-lasting anemia and hepatosplenomegaly with extramedullary hematopoiesis.**

- A Representative images of the spleen at day 14 after live *A. m.* or *A. m.* lysate injection.  
 B Spleen weight at day 14 after live *A. m.* or *A. m.* lysate injection † indicates death ( $n = 3$  biological replicates).  
 C Representative images of the spleen at day 14 after *A. m.* or *Bacteroides thetaiotaomicron* (*B.t.*) injection. Scale bars indicate 1 cm.  
 D Spleen weight (left) and total cell number (right) at day 14 after *A. m.* or *B. t.* injection ( $n = 3$ –4 biological replicates).  
 E Total nucleated cell number of splenocytes after PBS or *A. m.* injection ( $n = 4$ –16 biological replicates).  
 F, G Representative FACS plots (F) and frequency (G) of mature hematopoietic cells in the spleen (SPL) 14 days after PBS or *A. m.* injection ( $n = 12$ –13 biological replicates).  
 H, I Representative FACS plots (H) and frequency (I) of HSPC subpopulation (LK, LSK, and CLP) in total cells in the spleen at 14 days after PBS or *A. m.* injection ( $n = 5$ –8 biological replicates).  
 J Representative images of the spleen from PBS (left)- or *A. m.* (right)-treated  $Hlf^{tdTomato+}$  mice at day 14 (c-Kit, green; tdTomato, red; DAPI, blue). Arrowheads indicate putative HSCs (c-Kit<sup>+</sup>tdTomato<sup>-</sup>). Scale bars indicate 500  $\mu$ m.  
 K c-Kit<sup>+</sup> cells (left) and c-Kit<sup>+</sup>tdTomato<sup>+</sup> cells (right) in the spleen images from PBS- or *A. m.*-treated  $Hlf^{tdTomato+}$  mice at day 14 ( $n = 10$  biological replicates).  
 L Spleen weight and total cell number of splenocytes at day 14 after *A. m.* injection via *i.p.* vs. *i.v.* routes ( $n = 3$  biological replicates).

Data information: \* $P < 0.05$ , \*\* $P < 0.01$ , \*\*\* $P < 0.001$ , \*\*\*\* $P < 0.0001$  (two-tailed t-test), # $P < 0.05$ , ## $P < 0.01$ , ### $P < 0.001$ , #### $P < 0.0001$  (One-way ANOVA with Turkey's multiple comparisons or Two-way ANOVA with Šidák's multiple comparisons test). N.S., not significant. Error bars indicate SEM.

Source data are available online for this figure.

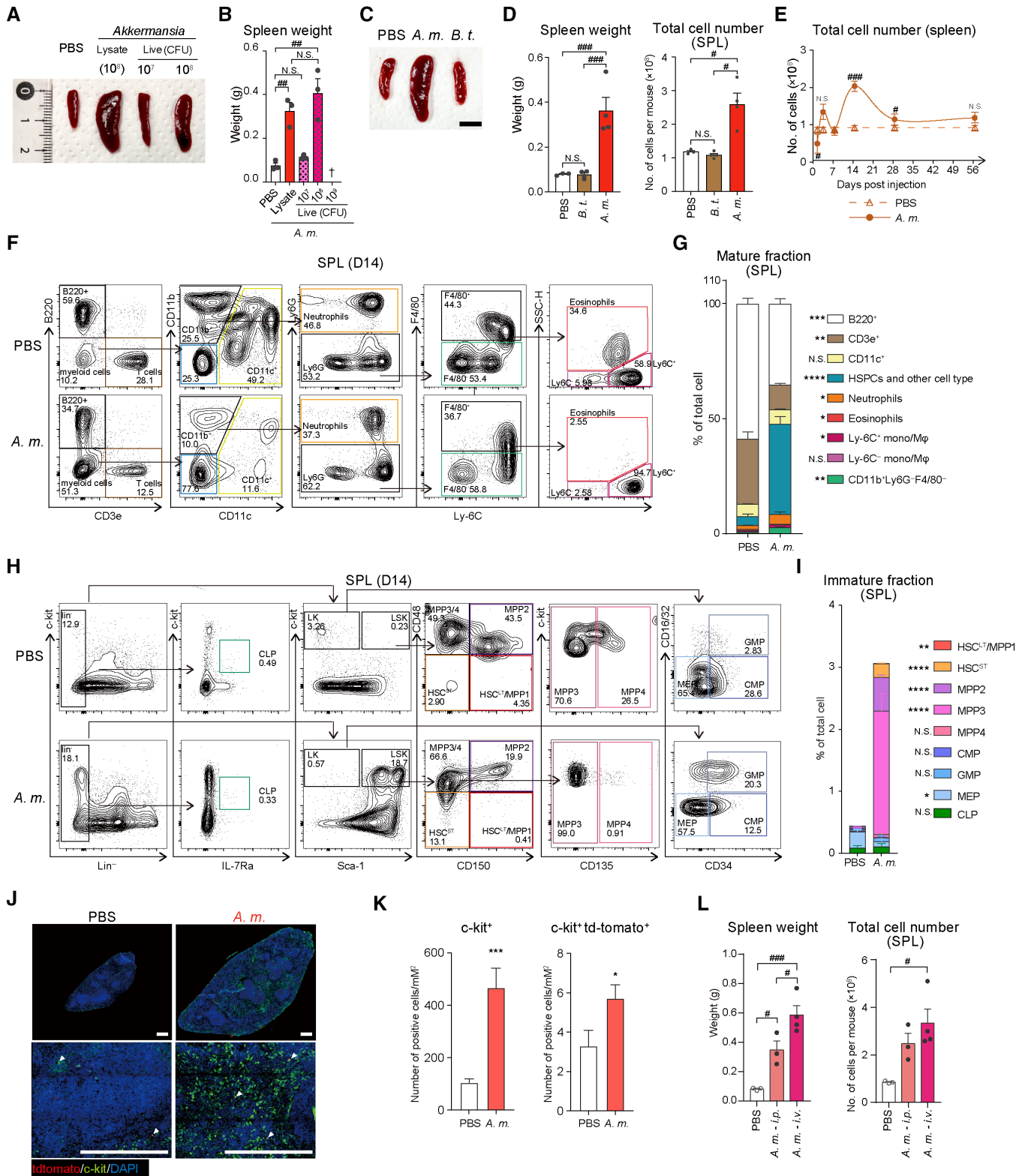


Figure 1.

control vs.  $39.97 \pm 4.31\%$  in *A. m.*-injected group). This was not observed in the BM ( $22.40 \pm 3.23\%$  in control vs.  $25.50 \pm 3.70\%$  in *A. m.*-injected group; Appendix Fig S1F and G).

The spleen is a site for EMH in response to systemic infection or other stresses, as it has previously been reported that HSPCs are mobilized to the spleen upon injection of live *Escherichia coli* or its

membrane components, as well as upon infiltration of the microbiota induced by colitis (Esplin *et al*, 2011; Griseri *et al*, 2012; Burberry *et al*, 2014). Thus, we hypothesized that long-term-sustained EMH would be driven by the mobilization and expansion of HSPCs in the spleen. Here, we defined Lin<sup>-</sup>Sca-1<sup>+</sup>c-Kit<sup>+</sup> cells (LSK) as HSPCs that include LT-HSC, ST-HSC, and multipotent progenitors (MPP1-4) by flow cytometry (Appendix Fig S1H). The frequency of HSPCs increased significantly in *A. m.*-injected mice compared to controls at day 14 post-injection ( $P < 0.001$ ,  $0.44 \pm 0.06\%$  in control vs.  $3.06 \pm 0.32\%$  of live cells in *A. m.*-injected spleen; Fig 1H and I), which was also observed in live *A. m.*-injected spleen, but not in *B. t.*-injected spleen (Appendix Fig S1I–K). In contrast, the total cell number of *A. m.*-treated BM decreased significantly with a slight change in the frequency of Lin<sup>-</sup> fractions at day 14 ( $2.32 \pm 0.16\%$  in control vs.  $3.41 \pm 0.31\%$  in *A. m.*-injected group; Appendix Fig S1L and M). Within the Lin<sup>-</sup> fraction, LSK cells containing HSCs and MPPs, both of which have self-renewal and multi-lineage differentiation potential, significantly expanded in *A. m.*-injected BM and spleen (Fig 1H and I, and Appendix Fig S1L and M). Supporting this data, immunofluorescent imaging of the spleen of *Hlf*<sup>tdTomato</sup> mice, that allow to visualize putative HSPC (Yokomizo *et al*, 2019) showed marked expansion of c-Kit<sup>+</sup>tdTomato<sup>+</sup> HSPCs and Gr-1<sup>+</sup>/Ly6G<sup>+</sup> mature myeloid cells in the red pulp of *A. m.*-injected spleen compared with controls (Fig 1J and K, and Appendix Fig S1N).

Our previous work as well as other reports showed that microbiota and their compounds increased in the blood due to the increased permeability of the intestinal barrier (Gracey *et al*, 2020; Kovtonyuk *et al*, 2021; Sezaki *et al*, 2022). We compared different injection routes of *A. m.* treatment. Intravenous (*i.v.*) injection of *A. m.* induced slightly bigger splenomegaly (Fig 1L) and comparable HSPC expansion both in the spleen and BM (Appendix Fig S1O), suggesting that the splenomegaly was induced by *A. m.* irrespective of the injection route.

Collectively, these data indicate that a single shot of *A. m.* induced significant hematopoietic responses characterized by long-term-sustained anemia and hepato-splenomegaly with EMH.

### Time-course kinetic analysis reveals two differential HSPC waves in *A. m.*-injected spleen

To characterize the long-term, sustained splenomegaly upon *A. m.* injection, time-course kinetics of HSPC populations were analyzed. The LSK fraction showed rapid increase in the BM as well as PB within 3 days after *A. m.* injection, accompanied by a slight increase of the spleen size. This was due to HSPC mobilization

(Fig 2A and B) that leads to a transient increase of HSPCs at day 3 (Fig 2C). The “first wave” of HSPC-containing LSK increase in the BM and PB appeared to cease within a week as shown by the frequency of LSK cells back to the baseline level by day 7 (Fig 2A and B). Subsequently, the Lin<sup>-</sup>Sca-1<sup>-</sup>c-Kit<sup>+</sup> (LK) fraction containing myeloid lineage-committed progenitors without self-renewal potential (Akashi *et al*, 2000) gradually increased in the spleen ( $4.92 \pm 1.66\%$  in control vs.  $18.64 \pm 1.72\%$  in *A. m.*-injected group) and reached its peak at day 7, followed by their differentiation into mature myeloid cells (Ly6C<sup>+</sup> monocyte, CD11c<sup>+</sup> cells, neutrophils) peaking at day 14 (Fig 2D and Appendix Fig S2A). After the “first wave”, a delayed but stronger “second wave” of HSPC increase (called delayed EMH thereafter) was observed with a peak at day 14 in *A. m.*-injected spleen ( $0.56 \pm 0.14\%$  in control vs.  $23.08 \pm 2.27\%$  in *A. m.*-injected group) and BM ( $2.14 \pm 0.15\%$  in control vs.  $18.90 \pm 2.18\%$  in *A. m.*-injected group; Fig 2A and B), but it gradually returned back to the baseline by day 56 (Fig 2C and D, and Appendix Fig S2B and C). Unlike the spleen, the mature myeloid fraction, especially eosinophils and Ly6C<sup>+</sup> monocytes in BM, along with the total cell number, showed a decrease at day 14 (Appendix Fig S2D).

One of the HSPC defining markers, Sca-1 (Essers *et al*, 2009) is the interferon (IFN)-responsive genes known to be upregulated upon bacterial infection (Essers *et al*, 2009), and may cause overestimation of HSPC number (Umemoto *et al*, 2017) due to a contamination of Sca-1 negative LK into LSK cells (Umemoto *et al*, 2017). Thus, we quantified HSPC using CD86 that has been recently reported as a surrogate HSPC marker under infection-stressed conditions (Kanayama *et al*, 2020), at day 1 and day 14 after *A. m.* injection (Fig 2E and F, and Appendix Fig S2E and F), and confirmed a comparable HSPC number in both definitions.

Collectively, these data indicate two distinct waves of HSPC expansion, a quick-responsive “first wave” and a delayed but long-lasting “second wave” in *A. m.*-injected spleen.

### *A. m.*-expanded HSCs in the spleen are transplantable

Functional HSCs are detectable in the spleen in steady-state and under stress conditions (Morita *et al*, 2011; Burberry *et al*, 2014). To examine whether HSCs that accumulated in *A. m.*-stimulated spleen are functional, we performed a competitive transplantation assay (Fig 3A). At 14 days after *i.p.* treatment with either PBS or *A. m.* in WT mice (CD45.1<sup>+</sup>),  $3 \times 10^5$  WBM (whole bone marrow, estimated to contain  $34.70 \pm 11.50$  of HSC<sup>LT</sup>/MPP1 in PBS-treated BM vs.  $34.40 \pm 1.81$  in *A. m.*-treated BM) and  $1 \times 10^6$  splenocytes (containing  $12.0 \pm 2.42$  of HSC<sup>LT</sup>/MPP1 in PBS-treated spleen vs.

**Figure 2. Time-course kinetic analysis reveals two distinct waves of HSPC increase in the *Akkermansia muciniphila*-injected spleen.**

- A, B Representative FACS plots of Lin<sup>-</sup> cells (A) and absolute number of LSK cells (B) in the BM (upper), spleen (middle), and PB (lower) at indicated timepoints after PBS or *A. m.* injection ( $n = 4–21$  biological replicates).
- C Absolute number of HSPC subfractions in the spleen of PBS or *A. m.*-injected mice ( $n = 4–22$  biological replicates).
- D Absolute number of CLP and LK subfractions within LSK in the spleen of PBS or *A. m.* injected mice ( $n = 4–22$  biological replicates).
- E, F Representative FACS plots (E) and the absolute number (F) of CD86- or Sca-1-defined HSPCs in the spleen at day 1 and 14 post PBS or *A. m.* injection ( $n = 4–7$  biological replicates).

Data information: <sup>#</sup> $P < 0.05$ , <sup>##</sup> $P < 0.01$ , <sup>###</sup> $P < 0.001$ , <sup>####</sup> $P < 0.0001$  (Two-way ANOVA with Šidák's multiple comparisons test). N.S., not significant. Error bars indicate SEM.

Source data are available online for this figure.

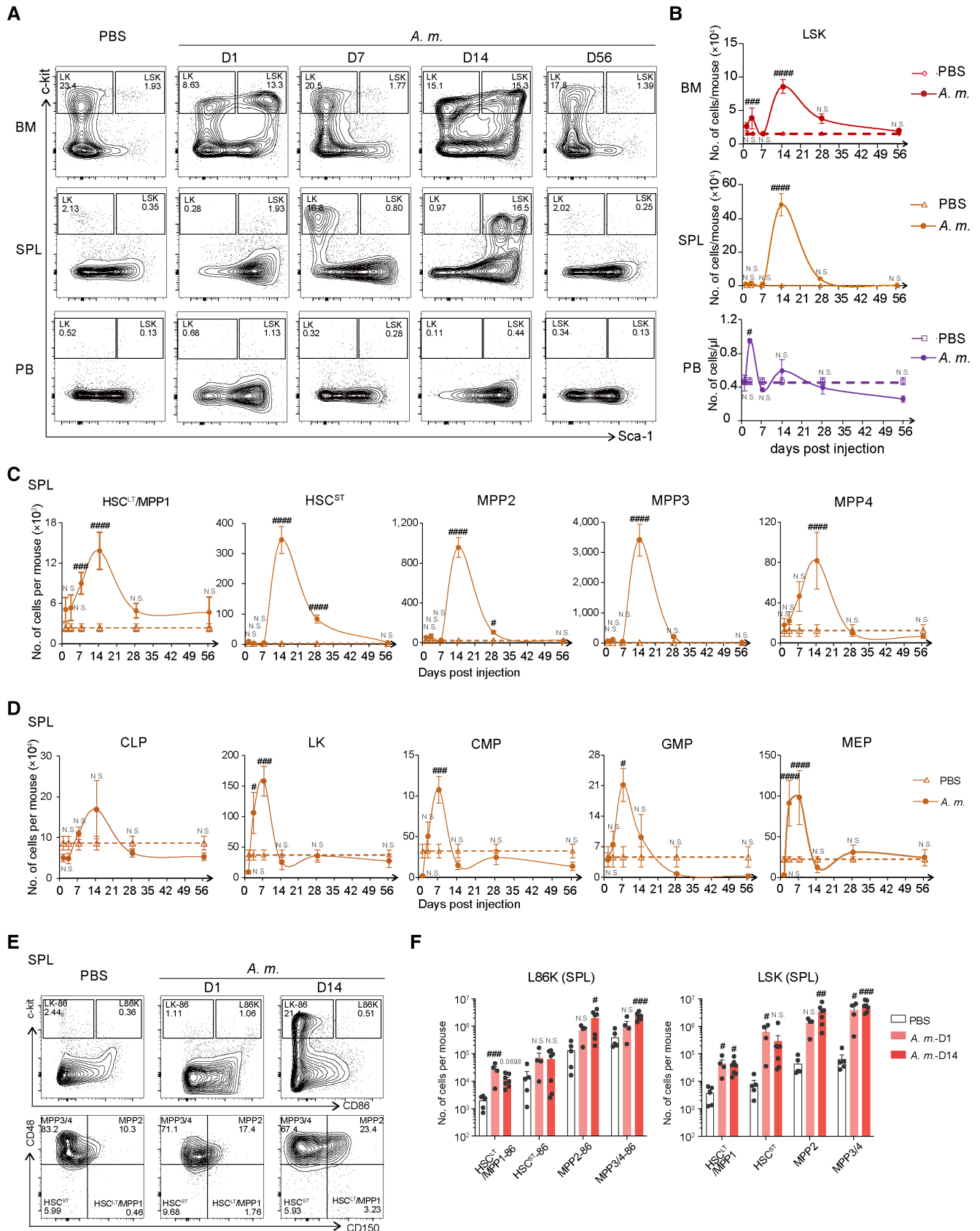


Figure 2.

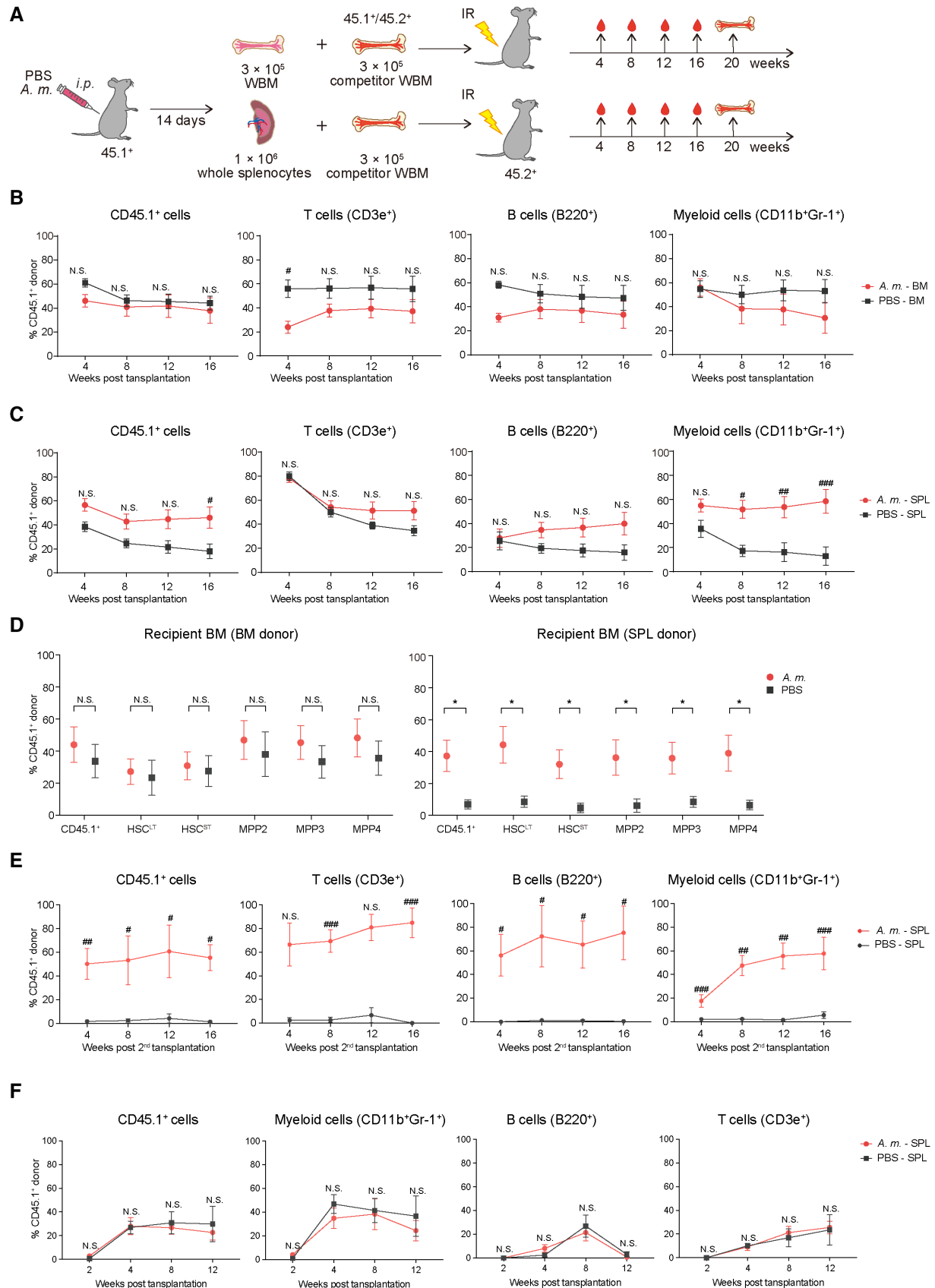


Figure 3.

**Figure 3. *Akkermansia muciniphila*-expanded HSCs in the spleen are transplantable.**

- A Experimental scheme of competitive transplantation:  $3 \times 10^5$  whole bone marrow (WBM) cells or  $1 \times 10^6$  whole splenocytes were isolated from PBS or *A. m.*-treated WT mice (CD45.1<sup>+</sup>) at day 14 post injection, mixed with  $3 \times 10^5$  WBM competitors (CD45.1/CD45.2<sup>+</sup>) and transplanted into lethally-irradiated (10Gy) WT mice (CD45.2<sup>+</sup>). Donor chimerism in the PB was analyzed monthly for up to 16 weeks and the BM for 20 weeks.
- B, C Time course kinetics of donor chimerism in the PB of recipients transplanted with whole BM (B) or splenocytes (C). Shown are donor chimerism of leukocytes (CD45.1<sup>+</sup>), myeloid (CD11b<sup>+</sup>Gr-1<sup>+</sup>), B-lineage (B220<sup>+</sup>), and T-lineage (CD3e<sup>+</sup>) cells ( $n = 7$ –11 biological replicates).
- D Donor chimerism in HSPCs from the BM of recipients transplanted with whole BM (left) or splenocytes (right) ( $n = 7$ –11 biological replicates).
- E Time course kinetics of donor chimerism in the PB of 2<sup>nd</sup> recipients transplanted with whole BM cells of 1<sup>st</sup> recipients ( $n = 3$ –5 biological replicates).
- F Time course kinetics of donor chimerism in the PB of recipients transplanted with 50 splenic HSC ( $n = 5$ –7 biological replicates).

Data information: \* $P < 0.05$  (two-tailed *t*-test). # $P < 0.05$ , ## $P < 0.01$ , ### $P < 0.001$  (Two-way ANOVA with Šidák's multiple comparisons test). N.S., not significant. Error bars indicate SEM.

Source data are available online for this figure.

84.25 ± 18.25 in *A. m.*-treated spleen) were transplanted into lethally-irradiated WT recipient mice (CD45.2<sup>+</sup>), together with  $3 \times 10^5$  WBM competitors from untreated WBM (CD45.1<sup>+</sup>CD45.2<sup>+</sup>; Appendix Table S1). Monthly donor chimerism assessment of the PB revealed that *A. m.*-treated WBM donors showed multilineage reconstitution comparable to that of PBS-treated controls over 4 months post transplantation (Fig 3B). However, *A. m.*-treated splenocytes showed significantly higher engraftment levels in total hematopoietic cells (CD45<sup>+</sup>) and myeloid lineage cells (CD11b<sup>+</sup>Gr-1<sup>+</sup>) but not in B or T cells (Fig 3C). This was further confirmed by terminal BM analysis of recipients at 5 months post transplantation, which showed a significantly higher donor chimerism in HSC<sup>LT</sup> fraction (6.89 ± 2.93% in PBS group vs. 37.34 ± 9.35% in *A. m.* group, 5.41 folds more in *A. m.* group; Fig 3D and Appendix Table S2). In contrast, no significant differences could be observed in WBM donor transplants (33.73 ± 10.36% in PBS group vs. 44.03 ± 11.11% in *A. m.* group). Serial transplantation of WBM cells derived from primary recipient mice revealed that only the *A. m.*-treated splenocytes group could reconstitute hematopoiesis in the secondary recipients, whereas untreated control splenocytes did not (Fig 3E). These data indicate that functionally transplantable HSCs possibly with myeloid-biased lineage output expanded numerically in the spleen at day 14, after one shot of systemic *A. m.* lysate injection.

To confirm whether the increased donor HSC chimerism was not due to enhanced self-renewal potential of HSCs from *A. m.*-injected spleen, we sorted 50 splenic LSKCD48<sup>-</sup>CD150<sup>+</sup> cells from spleen that had been previously stimulated with PBS control or *A. m.*, and performed co-transplantation with  $2 \times 10^5$  competitor WBM cells. The donor chimerism in peripheral blood showed no differences, suggesting that function of HSC did not change post *A. m.* stimulation (Fig 3F). Taken together, *A. m.* stimulation expands HSC number without affecting their function.

#### ***A. m.*-induced HSPC accumulation in the spleen is partially mediated by TLR2/4 and entirely by MYD88/TRIF dependent signals**

*Akkermansia muciniphila* is known to induce intestinal adaptive immune response (Ansaldò et al, 2019) and T cell activation (Derosa et al, 2022). To test the involvement of acquired immunity in *A. m.*-induced EMH, mice that lack B, T and NK cells (Saito et al, 2016) and are thereby immune-compromised for acquired immunity were challenged with PBS or *A. m.* lysate and analyzed 14 days later (Appendix Fig S3A). They showed intact splenomegaly and delayed EMH in response to *A. m.* lysate injection as good as

control Balb/c mice (Appendix Fig S3B–E). We also observed a comparable increase of spleen weight, total cell number, and the cell number of splenic LSKs in acquired immunity-deficient mice to that of control mice (Appendix Fig S3F), indicating little contribution of adaptive immunity to this phenotype.

*Akkermansia muciniphila* is a gram-negative bacterium with lipopolysaccharide (LPS; Plovier et al, 2017), a membrane component that can activate and mobilize HSCs directly through the Toll-like receptor (TLR) 4-signaling pathway (Burberry et al, 2014; Liu et al, 2022). The purified membrane protein, Amuc\_1100 isolated from the *A. m.* has been reported to bind to TLR2 (Plovier et al, 2017). Therefore, we next tested whether *A. m.* is able to recruit HSPCs in the spleen via TLRs. *Tlr2;4<sup>-/-</sup>* double knock out (DKO) mice lacking TLR2 and TLR4 expression and *Myd88;Trif<sup>-/-</sup>* DKO mice lacking the down-stream adaptor molecules of TLR and IL-1R signaling were challenged with PBS or *A. m.* (Fig 4A). The severe hepato-splenomegaly with little or no HSPC accumulation in the spleen and BM that occurred in WT mice was partially and completely canceled in *Tlr2;4<sup>-/-</sup>* DKO and *Myd88;Trif<sup>-/-</sup>* DKO, respectively (Fig 4B–E and Appendix Fig S3G–I). These results indicate that *A. m.*-induced EMH is partially dependent on TLR2/4-mediated signals but completely dependent on MYD88/TRIF-mediated signals.

To further confirm splenomegaly-inducing signals, LPS and Pam3CSK4, a ligand for TLR4 and TLR2 agonists, respectively, were *i.p.* injected into WT mice and compared to the same dosage of *A. m.* (Fig 4F). Although a single shot of Pam3CSK4 induced a mild splenomegaly at day 1, neither LPS nor Pam3CSK4 could induce the delayed splenomegaly and HSPC accumulation in the spleen and BM. at day 14 (Fig 4G–I). Additionally, the combination of LPS and Pam3CSK4 also failed to trigger splenomegaly (unpublished observation by the authors).

Taken together, these data suggest that although TLR2/4 signals partially contribute to splenomegaly, additional TLR2/4 independent innate immune signals are required for triggering *A. m.*-induced splenomegaly.

#### **Sustained secretion of IL-1α mainly by splenic myeloid cells contributes to TLR2/4-independent delayed EMH**

Since other TLRs are also involved in MYD88/TRIF-mediated pathways (Akira & Takeda, 2004; Takizawa et al, 2017) and proinflammatory cytokines, such as IL-1 (Pietras et al, 2016), IFNs (Essers et al, 2009; MacNamara et al, 2011), tumor necrosis factor-α (TNF-α; Yamashita & Passegue, 2019) affect HSC fate and blood cell

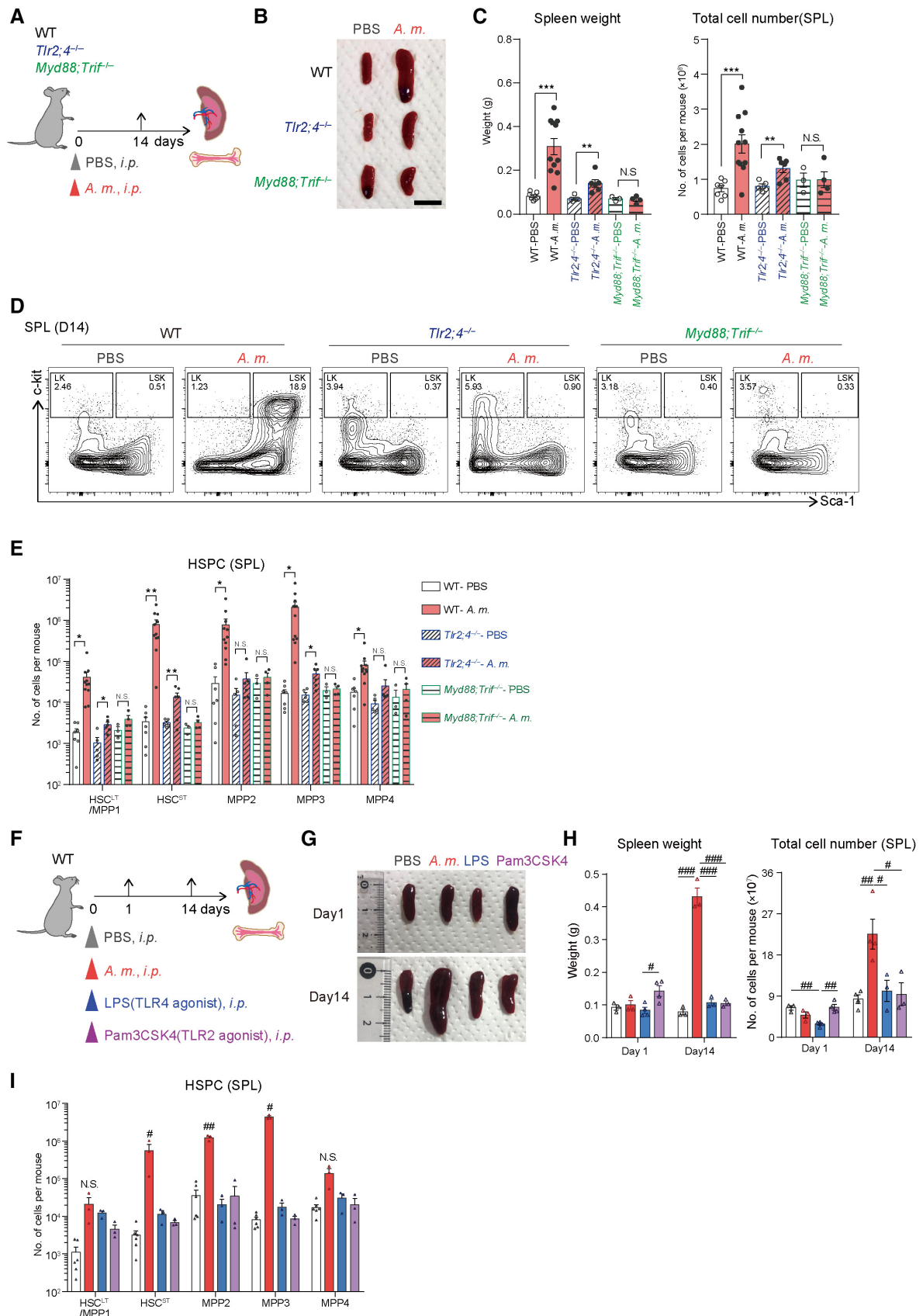


Figure 4.



**Figure 4. *Akkermansia muciniphila*-induced splenic HSPC expansion is mediated by innate immune signals, partially by TLR2/4 signals.**

- A Experimental scheme of *A. m.* injection into WT vs. innate immune signal-deficient mice: WT, *Tlr2;4* or *Myd88;Trif* DKO mice were *i.p.* treated with PBS or *A. m.* and the spleen and BM were analyzed at day 14 post injection.
- B Representative images of the spleen. Scale bar indicates 1 cm.
- C Spleen weight (left) and total cell number (right) of splenocytes from WT mice treated with PBS (WT-PBS) or *A. m.* (WT-*A. m.*), *Tlr2;4* DKO mice injected with PBS (*Tlr2;4* DKO-PBS) or *A. m.* (*Tlr2;4* DKO-*A. m.*), or *Myd88;Trif* DKO mice injected with PBS (*Myd88;Trif* DKO-PBS) or *A. m.* (*Myd88;Trif* DKO-*A. m.*;  $n = 4-11$  biological replicates) WT, *Tlr2;4* or *Myd88;Trif* DKO mice treated with PBS or *A. m.*
- D Representative FACS plots of Lin<sup>-</sup> splenocytes from PBS or *A. m.*-treated WT, *Tlr2;4* or *Myd88;Trif* DKO mice.
- E Absolute number of splenic HSPC subpopulations of WT mice injected with PBS (WT-PBS) or *A. m.* (WT-*A. m.*), *Tlr2;4* DKO mice injected with PBS (*Tlr2;4* DKO-PBS) or *A. m.* (*Tlr2;4* DKO-*A. m.*), or *Myd88;Trif* DKO mice injected with PBS (*Myd88;Trif* DKO-PBS) or *A. m.* (*Myd88;Trif* DKO-*A. m.*) ( $n = 4-11$  biological replicates).
- F Experimental scheme of *A. m.* vs. TLR agonist treatment: WT mice were *i.p.* injected with PBS, 200  $\mu$ g *A. m.*, 200  $\mu$ g LPS or 200  $\mu$ g Pam3CSK4, and the spleen and BM were analyzed 14 days later.
- G Representative images of the spleen treated with PBS, *A. m.*, LPS, or Pam3CSK4 at day 1 (upper) and 14 (lower) post injection.
- H Spleen weight at day 1 and 14 ( $n = 3-7$  from 6 independent experiments).
- I Absolute cell number of HSPC subpopulations of the spleen at day 14 ( $n = 4-7$  biological replicates).

Data information: \* $P < 0.05$ , \*\* $P < 0.01$ , \*\*\* $P < 0.001$  (two-tailed t-test). # $P < 0.05$ , ## $P < 0.01$ , ### $P < 0.001$ , (one-way ANOVA with Turkey's multiple comparisons). N.S., not significant. Error bars indicate SEM. Source data are available online for this figure.

output, we considered the possibility of inflammation-mediated EMH. We quantified various inflammatory factors in the serum, spleen fluid, BM, and spleen cell lysate isolated from *A. m.*-treated mice (Fig 5A–D and Appendix Fig S4A–D). Among all the cytokines measured, the concentration of IL-1 $\alpha$  showed a remarkable 25-fold increase at day 1 and 2-fold increase at day 14 in the spleen fluid and spleen cell lysate of *A. m.*-treated mice compared to their corresponding controls (Fig 5A and B, and Appendix Fig S4A). The elevation of IL-1 $\alpha$  in the spleen was partially reduced in *Tlr2;4*<sup>-/-</sup> DKO spleen and fully suppressed in *Myd88;Trif*<sup>-/-</sup> DKO spleen (Fig 5A and B), suggesting partial TLR2/4<sup>-</sup> and complete MYD88/TRIF-dependency of IL-1 $\alpha$  secretion in the spleen. In contrast, IL-1 $\alpha$  was unchanged in the serum and likewise, increased only at day 1 post *A. m.* stimulation in the BM (Fig 5C and Appendix Fig S4A). Therefore, its secretion appears restricted to the spleen. Although IL-1 $\beta$  and TNF- $\alpha$  also showed remarkable elevation in *A. m.*-treated spleen at day 1, their levels were not sustained for 2 weeks (Fig 5A and B, and Appendix Fig S4A). IFN- $\gamma$  showed a continuous increase over time in both the spleen and serum (Fig 5A and B, and Appendix Fig S4A and B). However, when *Stat1* KO mice that lacks IFN response (Umamoto *et al.*, 2017) were challenged with *A. m.*, they showed intact EMH response, suggesting its little contribution to the EMH (Unpublished observations). Measurement of G-CSF and CXCL12, both known as HSPC mobilization factors (Burberry

*et al.*, 2014) revealed transient upregulation of G-CSF in the serum and downregulation of CXCL12 in the BM fluid already at day 1 (Fig 5D, and Appendix Fig S4C and D). These results indicate that both G-CSF and CXCL12 trigger initial HSPC mobilization during the early phase (Fig 2A and B), but do not contribute to *A. m.*-induced delayed EMH.

To determine which cell fraction secretes IL-1 $\alpha$ , we designed a myeloid lineage-specific FACS panel that can separate myeloid cell fractions such as macrophages, granulocytes, eosinophils, pDCs (plasmacytoid dendritic cells), cDC1 (type 1 conventional dendritic cells), cDC2 (type 2 conventional dendritic cells), Ly6C<sup>+</sup> monocytes and Ly6C<sup>-</sup> monocytes, and use another panel for lymphocyte, megakaryocyte, and non-hematopoietic cells (CD45<sup>-</sup>; Appendix Fig S4E–G), and analyzed the expression of intracellular IL-1 $\alpha$  protein. All myeloid cells tested in the spleen expressed IL-1 $\alpha$ , whereas lymphoid cells and megakaryocytes showed no increased IL-1 $\alpha$  production (Fig 5E and F, and Appendix Fig S4H). CD45<sup>-</sup> fraction that contain non-hematopoietic cells such as stromal cells also showed an increase of IL-1 $\alpha$ <sup>+</sup> cells in day1 and day14 post *A. m.* treated spleen. Given around 80 and 10% of splenocytes are leukocytes and stroma respectively (Appendix Fig S4G and H), the major source of IL-1 $\alpha$  secretion is likely leukocyte. These results indicated that *A. m.*-triggered sustained high level of IL-1 $\alpha$  in the spleen was mainly secreted from myeloid cells.

**Figure 5. Sustained secretion of IL-1 $\alpha$  mainly from splenic myeloid cells contributes to TLR2/4-independent delayed EMH.**

- A, B Concentration of IL-1 $\alpha$ , IL-1 $\beta$ , TNF- $\alpha$ , and IFN- $\gamma$  in the spleen cell lysate (A) or spleen fluid (B) from WT, *Tlr2;4* or *Myd88;Trif* DKO mice treated with PBS or *Akkermansia muciniphila* at the indicated timepoint ( $n = 3-4$  biological replicates).
- C, D Concentration of IL-1 $\alpha$  (C), G-CSF in the serum and CXCL12 in the BM fluid (D) from WT mice treated with PBS or *A. m.* at day 1 and 14 ( $n = 3-6$  biological replicates).
- E, F Representative FACS dot plots (E) and percentage of IL-1 $\alpha$ <sup>+</sup> (F) in DCs, monocytes, macrophages, and neutrophils in the spleen at day 1, and 14 ( $n = 3-4$  independent experiments).
- G, H Representative FACS histogram in splenic LSK (G) and relative MFI of IL-1R expression in HSPCs of *A. m.*-treated mice to PBS-treated mice (H) in the spleen at day 14 ( $n = 6-8$  biological replicates).
- I Experimental scheme of *A. m.* injection into WT vs. IL-1 $\alpha$  KO mice.
- J, K Spleen weight (J) and absolute cell number of HSPC subpopulations in the spleen (K) at day 14 of WT and *Il-1 $\alpha$* <sup>-/-</sup> treated with PBS or *A. m.* (WT-*A. m.*, *Il-1 $\alpha$* <sup>-/-</sup>-*A. m.*). Dashed line indicates spleen weight and cell numbers in PBS-treated spleen ( $n = 5-6$  biological replicates).

Data information: \* $P < 0.05$ , \*\* $P < 0.01$ , \*\*\* $P < 0.001$ , \*\*\*\* $P < 0.0001$  (two-tailed t-test), # $P < 0.05$ , ## $P < 0.01$ , ### $P < 0.001$  (One-way ANOVA with Dunnett-t comparison or two-way ANOVA with Sidák's multiple comparisons test). N.S., not significant. Error bars indicate SEM. Source data are available online for this figure.

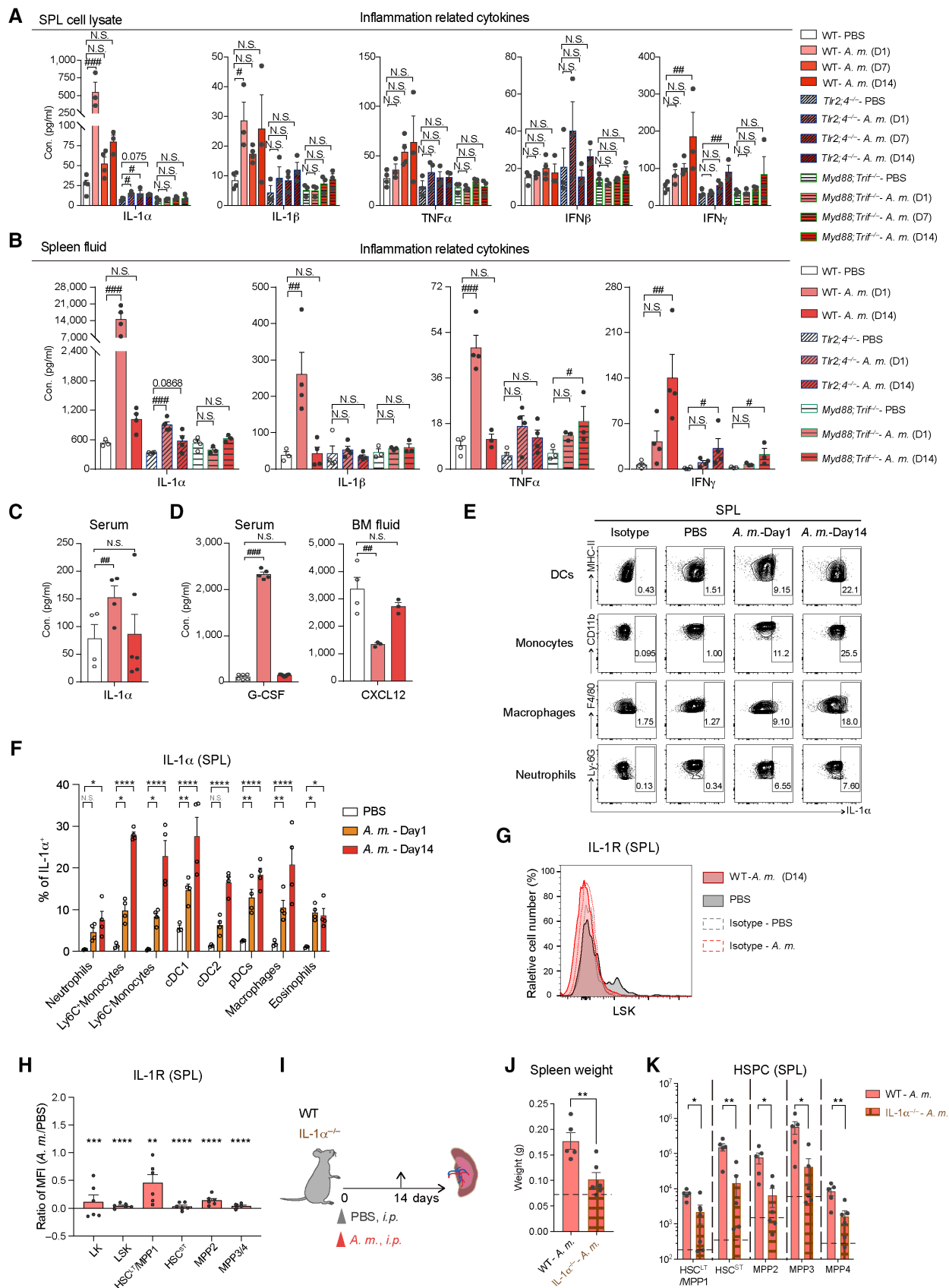


Figure 5.

Next, to determine which cells sense IL-1 $\alpha$  signal, we analyzed expression of its cognate receptor, IL-1RI in splenic mature cells and HSPCs. LSK cells express IL-1RI in steady state but dramatically downregulated its expression at day 14 after *A. m.* injection, especially in the spleen (Fig 5G and H, and Appendix Fig S4G and H). This is consistent with the fact that IL-1RI is known to be internalized upon binding of IL-1 $\alpha$  or IL-1 $\beta$  (Curtis et al, 1990; Cendrowski et al, 2016). Our data suggest that *A. m.* stimulation activates splenic DCs and inflammatory monocytes to produce IL-1 $\alpha$  locally and stimulate its cognate receptor expressed on LSK cells.

Since IL-1 $\alpha$  levels best correlated with splenomegaly and HSPC expansion in the spleen (Fig 5 and Appendix Fig S4A–J), it is likely that the remaining TLR2/4-independent hematopoietic responses are mediated by IL-1 $\alpha$  signaling. We tested this hypothesis using *Il-1 $\alpha$ <sup>-/-</sup>* mice (Fig 5I). The *A. m.*-induced splenomegaly and HSPC expansion were significantly inhibited in *Il-1 $\alpha$ <sup>-/-</sup>* mice (Fig 5J and K, and Appendix Fig S4K and L), indicating a major role of IL-1 $\alpha$  for *A. m.*-induced EMH. Since macrophage is one of the IL-1 $\alpha$  producers (Fig 5E and F), we depleted them by injecting clodronate liposomes. However, mice treated with clodronate and *A. m.* showed significantly increased spleen size/weight and EMH response compared to the clodronate-PBS-treated group, although the response was slightly reduced compared to control liposome group (Appendix Fig S4M–P), indicating little contribution of macrophage-produced IL-1 $\alpha$ .

To test if blocking of both TLR and IL-1R pathways can cancel *A. m.*-induced EMH, we administered human IL-1R antagonist (hIL-1ra), Anakinra, daily over 2 weeks to WT, *Tlr2;4<sup>-/-</sup>* and *Myd88;Trif<sup>-/-</sup>* DKO mice following *A. m.* injection (Fig 6A). Anakinra treatment resulted in a significant reduction of splenomegaly and the total cell number in both mouse strains, close to WT (ca. 59.0% reduction of spleen weight in WT-*A. m.* + hIL-1ra vs. WT-*A. m.*, while 86.6% reduction in *Tlr2;4<sup>-/-</sup>* - *A. m.* vs. WT-*A. m.*; Fig 6B and C). Detailed analysis showed a decrease of myeloid lineage cells, especially splenic DCs and Ly6C<sup>+</sup> monocytes which decreased neatly to the baseline level in *Tlr2;4<sup>-/-</sup>* DKO mice treated with Anakinra (Fig 6D and Appendix Fig S5A). Accumulation of HSPC and myeloid cells in the spleen were partially reduced in WT mouse and almost completely canceled in *Tlr2;4<sup>-/-</sup>* DKO mice (ca. 48.8% reduction of HSPC population in *Tlr2;4<sup>-/-</sup>*-*A. m.* + hIL-1ra vs. *Tlr2;4<sup>-/-</sup>*-*A. m.*). These data indicate that cooperative IL-1R- and TLR2/4-mediated signals contribute to *A. m.*-induced delayed EMH (Fig 6E and F). Of note, normalization of HSPCs by IL-1 inhibition was found only in the spleen but not in the BM (Appendix Fig S5B

and C), which again confirms local IL-1 $\alpha$  signaling as key in the spleen.

Collectively, these data suggest sustained local IL-1 $\alpha$  production in the spleen upon *A. m.* treatment is regulated partly by TLR2/4, together with MYD88/TRIF signals, and cooperative interplay between TLR2/4 and IL-1R is required for local HSPC and myeloid cell expansion, ultimately leading to delayed EMH.

## Discussion

This study demonstrates that a single injection of *A. m.*-derived agents triggers a series of hematopoietic responses leading to chronic splenomegaly, sustained by two temporally distinct waves of EMH (Fig 7). At day 1 post *A. m.* injection, HSPCs rapidly increase in the BM and are mobilized to the PB via upregulation of G-CSF in the serum and downregulation of CXCL12 in the BM (Fig 5D). The spleen showed pancytopenia and local production of IL-1 $\alpha$  for emergency hematopoiesis (Figs 2A and B, and 5A and B). This “first wave” of HSPC expansion appears to cease by their gradual differentiation into myeloid lineage-committed progenitors at day 7, followed by the generation of mature myeloid cells including Ly6C<sup>+</sup> monocytes, DCs, and neutrophils by day 14 (Fig 2D and Appendix Fig S2A). After the “first wave” of EMH, a gradual but stronger “second wave” of HSPC expansion occurs at day 14 in the spleen and BM (Fig 2A and B). Chronic accumulation of HSPCs and their differentiation into mature myeloid cells result in sustained splenomegaly and long-term EMH. Moreover, we found that *A. m.* stimulation induced consistent local secretion of IL-1 $\alpha$  in the spleen which partially contributes to delayed EMH.

Mechanistically, our data indicates that delayed EMH is dependent on downstream MYD88/TRIF signaling pathways, cooperatively mediated by TLR2/TLR4 and IL-1R signals (Figs 5–7). Sustained secretion of IL-1 $\alpha$  mainly from splenic myeloid cells stimulate IL-1R-expressing LSK cells in spleen and contribute to delayed EMH. The acute local secretion of IL-1 $\alpha$  in the spleen appears largely dependent on TLR2/TLR4 signaling, but its remaining chronic expression depends on other pathways than TLR2/4, which is mediated by MYD88/TRIF signaling (Fig 5A and B). This is supported by the fact that administration of either Pam3CSK4 or LPS alone was not sufficient to recapitulate delayed EMH (Fig 4F–I). In contrast to previous reports stating that chronic LPS or IL-1 $\beta$  stimulation damages HSC function (Esplin et al, 2011; Pietras et al, 2016), we did not see any obvious dysfunction in HSC transplantability (Fig 3), but increase number of functional HSCs. While the majority of

**Figure 6. Pharmacological inhibition of IL-1R and genetic ablation of TLR2/4 alleviates EMH.**

- A Experimental scheme of hIL-1ra treatment: WT, *Tlr2;4*, or *Myd88;Trif* DKO mice were treated with *Akkermansia muciniphila* followed by daily injections with or without hIL-1ra treatment. Spleen and BM were analyzed at day 14.
- B Representative images of the spleen from WT or *Tlr2;4* DKO treated with *A. m.*  $\pm$  hIL-1ra.
- C Spleen weight (left) and total cell number (right) of splenocytes at day 14 ( $n = 3$ –7 biological replicates). Dashed line indicates spleen weight and cell numbers in PBS-treated spleen.
- D Absolute cell number of splenic DCs and Ly6C<sup>+</sup> monocytes at day 14 ( $n = 3$ –7 biological replicates). Dashed line indicates absolute cell numbers in PBS-treated spleen.
- E, F Representative FACS plots (E) and absolute cell number (F) of HSPC subpopulations in the spleen at day 14 ( $n = 3$ –6 biological replicates). Dashed lines indicate absolute cell numbers of each HSPC fractions in PBS-treated spleen.

Data information: \* $P < 0.05$ , \*\* $P < 0.01$ , \*\*\* $P < 0.001$ , \*\*\*\* $P < 0.0001$  (two-tailed t-test). N.S., not significant. Error bars indicate SEM. Source data are available online for this figure.

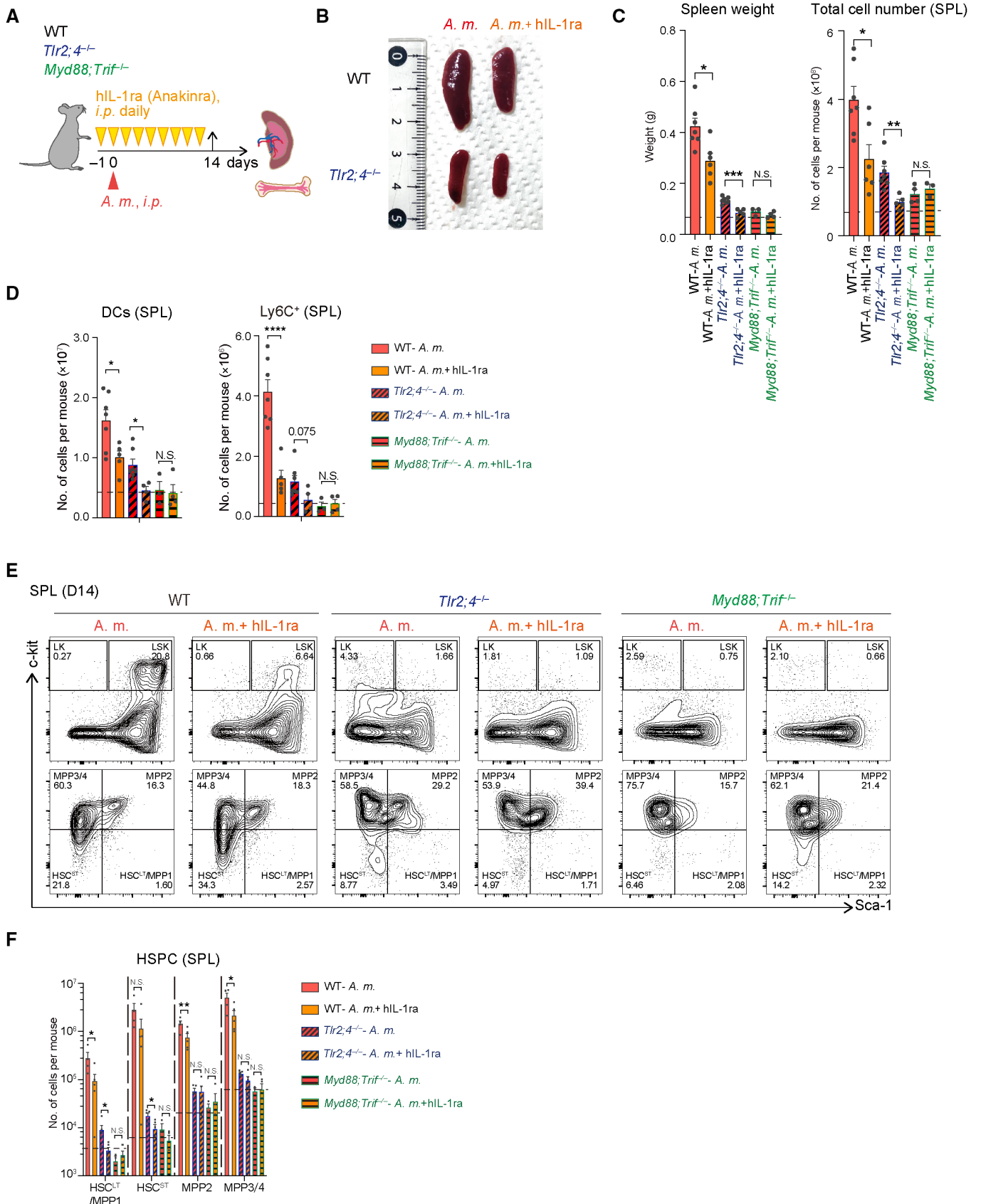
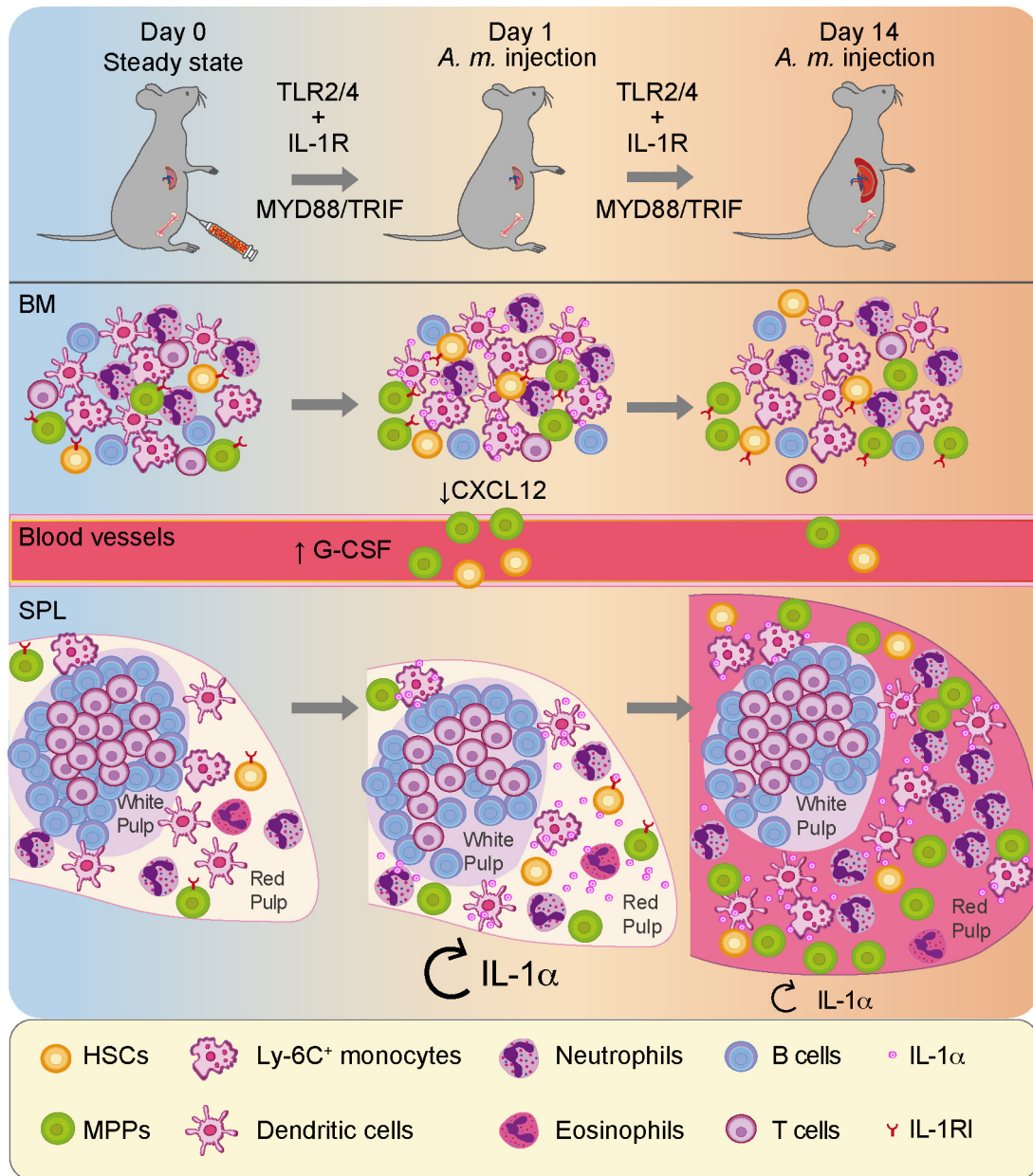


Figure 6.



**Figure 7. Extramedullary hematopoiesis is triggered by *Akkermansia muciniphila* injection.**

The schematic model shows how the hematopoietic system responds to *A. m.* infection. At day 1 post *A. m.* injection, CXCL12 in the BM is downregulated, while the secretion of G-CSF in the PB increases, and mobilizes HSPCs from the BM to spleen. Concurrently, IL-1 $\alpha$  secretion in the spleen is significantly elevated and drives expansion of HSCs that have migrated to the spleen and their differentiation into myeloid cells. At day 14 post *A. m.* injection, persistent secretion of IL-1 $\alpha$  and activation of TLR signals synergistically contribute to the constant expansion of functional HSPCs and their differentiation in spleen, ultimately leading to delayed EMH and splenomegaly.

splenocytes that expand chronically depends on TLR2/TLR4 signaling, only those that chronically expand depends on IL-1R signaling (Figs 5 and 6). However, what bacterial component in the *A. m.* lysate triggers delayed EMH response remains yet to be determined.

Extramedullary hematopoiesis occurs frequently during severe bacterial infection (Burberry *et al.*, 2014; Krishnan *et al.*, 2021), metabolic stress (Westertep *et al.*, 2012) and IBD (Griseri *et al.*, 2012), probably as a compensatory mechanism for ineffective BM

hematopoiesis. Although EMH can be found in many organs, the spleen is considered to be one of the most common sites. This is likely because (i) the spleen plays a central role in host defense to integrate both the innate and adaptive immune systems in an efficient way (Mebius & Kraal, 2005) and (ii) the spleen serves as a hematopoietic organ during embryonic development (Djaldetti *et al.*, 1972). Similar to the BM niche, there is increasing evidence supporting spleen stromal cell subsets as key regulators of organ

development and tissue regeneration (Golub *et al*, 2018), albeit the underlying molecular mechanism is still unknown. Upon pathological EMH triggered by chemotherapy and G-CSF, SCF and CXCL12 secreted from splenic stromal cells are key regulators for EMH (Inra *et al*, 2015). Consistently, we also found elevation of both SCF and CXCL12 in the spleen at day 14 post *A. m.* injection (Appendix Fig S4C and D), suggesting the splenic niche was disturbed by *A. m.* Further study is necessary to address whether splenic niche cells secrete IL-1 $\alpha$  to regulate *A. m.*-induced delayed EMH, as we noticed that some CD45<sup>+</sup> cells could produce IL-1 $\alpha$ . Notably, we also found that other inflammatory factors such as MCP-1, also known as CCL2, increased in spleen lysate, BM lysate and serum at day 1. Since CCL2 is an integral chemotactic factor known to play a crucial role in recruiting monocytes from the bone marrow to various tissues including the spleen, in response to inflammation or injury (Lin *et al*, 2022), it may also recruit the myeloid cells to the inflammation site during acute phase post *A. m.* stimulation.

We found that late-onset delayed EMH in the spleen is mediated by innate immune signals, particularly TLR2/4 and IL-1R, with the latter possibly being regulated by local and persistent secretion of IL-1 $\alpha$  upon *A. m.* stimulation. To our knowledge, IL-1 $\alpha$ -mediated EMH has not yet been reported. Abnormal activation of IL-1 family members is commonly found in certain chronic autoimmune-diseases such as rheumatoid arthritis (RA), atherosclerosis, and systemic lupus erythematosus (SLE; Migliorini *et al*, 2020). In human RA patients, aberrant hematopoiesis such as chronic anemia (Papadaki *et al*, 2002a), myeloid expansion as well as immunosenescence (Papadaki *et al*, 2002b) are frequent causes for complications (Firestein, 2003). A subset of RA patients are

associated with leukocytopenia and splenomegaly, known as Felty's syndrome (Newman & Akhtari, 2011). This could be in part due to expansion of RA-derived HSCs that are myeloid-biased via IL-1R-mediated signals (Hernandez *et al*, 2020). Moreover, arthritis is frequently associated with IBD, a chronic inflammatory disorder highly related to intestinal barrier dysfunction and aberrant commensal microbiota distribution (Rogler *et al*, 2021). *A. m.* is a mucin-degrading bacterium which might infiltrate into the circulation upon gut tissue damage. A recent publication identified one specific lipid, a diacyl phosphatidylethanolamine of *A. m.* that could trigger a release of inflammatory cytokines through a non-canonical TLR2–TLR1 heterodimer, to regulate human immune response (Bae *et al*, 2022). TLR2 composes TLR1/2, TLR2/6 heterodimers and TLR2 homodimer, while TLR4 has a homodimer. Thus, it remains possible that TLR1 may also play a role in the development of splenomegaly by recognizing microbial-associated molecular patterns (MAMPs) and activating the pro-inflammatory signaling in concert with TLR2 (Li *et al*, 2013). All these suggest a relationship between *A. m.* and RA-associated EMH that might be worth to study in the future. Ours and other findings highlight that the cross-talk between multiple organs, or even horizontal interaction between different organisms, e.g., microbiome and host, may play a crucial role in the development of various immune-related diseases.

In conclusion, systemic stimulation with the membrane fraction of *A. m.*, one of the most abundant mucin-associated microbiota involved in various human pathologies, induced late-onset EMH through TLR2/4 and IL-1R. These novel findings might be involved in the pathogenesis of IL-1-related autoimmune diseases and may lead to the development of novel therapies for their treatment.

## Materials and Methods

### Reagents and Tools table

Reagent/Resource	Reference or Source	Identifier or Catalog Number
<b>Experimental Models</b>		
<i>Akkermansia muciniphila</i> ATCC BAA-835	Riken	JCM 33894
<i>Mus musculus</i> : C57Bl/6J	Japan SLC/Jackson Laboratories	Wildtype mouse line – CD45.2 RRID: IMSR_JAX:000664
<i>Mus musculus</i> : BALB/cCrSlc	Japan SLC	Wildtype mouse line – CD45.2 RRID: MGI:2161019
<i>Mus musculus</i> : Hlf <sup>tdTomato+</sup>	Yokomizo <i>et al</i> (2019) <i>J Exp Med</i>	
<i>Mus musculus</i> : Tlr2 <sup>-/-</sup> ;Tlr4 <sup>-/-</sup>	Oriental BioService	IMSR_OBS:19
<i>Mus musculus</i> : Trif <sup>-/-</sup> ;Myd88 <sup>-/-</sup>	Oriental BioService	IMSR_OBS:22
<i>Mus musculus</i> : MSTRG	Rongvaux <i>et al</i> (2014), <i>Nat Biotechnol</i>	
<i>Mus musculus</i> : Il-1 $\alpha$ <sup>-/-</sup>	Horai <i>et al</i> (1998), <i>J Exp Med</i>	
<i>Mus musculus</i> : CD45.1	Japan SLC/Jackson Laboratories	
<b>Recombinant DNA</b>		
<b>Antibodies</b>		
Rat anti-mouse B220-FITC (RA3-6B2)	BioLegend	103205 (1:100) RRID: AB_312990
Rat anti-mouse B220-Biotin (RA3-6B2)	BioLegend	103204 (1:500) RRID: AB_312989
Armenian hamster anti-mouse CD3e-PE-Cy5 (145-2C11)	BioLegend	100310 (1:50) RRID: AB_312675
Armenian hamster anti-mouse CD3e-Biotin (145-2C11)	BioLegend	100304 (1:500) RRID: AB_312669

Reagents and Tools table (continued)

Reagent/Resource	Reference or Source	Identifier or Catalog Number
Rat anti-mouse F4/80-PE (BM8)	Thermo Fisher Scientific	12-4801-82 (1:100) RRID: AB_465923
Rat anti-mouse Gr-1-BV510 (RB6-8C5)	BioLegend	108438 (1:100) RRID: AB_2562215
Rat anti-mouse Gr-1-Biotin (RB6-8C5)	BioLegend	108404 (1:500) RRID: AB_313369
Rat anti-mouse Ly-6G-AF647 (1A8)	BioLegend	127610 (1:100) RRID: AB_1134159
Rat anti-mouse Ly-6C-AF700 (HK1.4)	BioLegend	128024 (1:100) RRID: AB_10643270
Armenian hamster anti-mouse CD11c-PE-Cy7 (N418)	BioLegend	117318 (1:100) RRID: AB_493568
Rat anti-mouse CD11b-APC-Cy7 (M1/70)	BioLegend	101226 (1:50) RRID: AB_830642
Rat anti-mouse CD11b-Biotin (M1/70)	BioLegend	101204 (1:500) RRID: AB_312787
Mouse anti-mouse CD45.1-PB (A20)	BioLegend	110722 (1:50) RRID: AB_492866
Mouse anti-mouse CD45.1-PE (A20)	BioLegend	110708 (1:50) RRID: AB_313497
Mouse anti-mouse CD45.2-PE (104)	BioLegend	109808 (1:50) RRID: AB_313445
Mouse anti-mouse CD45.2-APC (104)	BioLegend	109814 (1:50) RRID: AB_389211
Rat anti-mouse Ter-119-Biotin (TER-119)	BioLegend	116204 (1:500) RRID: AB_313705
Rat anti-mouse CD4-Biotin (GK1.5)	BioLegend	100404 (1:500) RRID: AB_312689
Rat anti-mouse CD8a-Biotin (53-6.7)	BioLegend	100704 (1:500) RRID: AB_312743
Rat anti-mouse NK1.1-Biotin (PK136)	BioLegend	108704 (1:500) RRID: AB_313391
Rat anti-mouse IL-7Ra-FITC (A7R34)	BioLegend	135008 (1:50) RRID: AB_1937232
Rat anti-mouse IL-7Ra-Biotin (SB/199)	BioLegend	121104 (1:500) RRID: AB_493502
Rat anti-mouse c-kit-PE-Cy7 (2B8)	BioLegend	105814 (1:100) RRID: AB_313223
Rat anti-mouse Sca-1-APC/Cy7 (D7)	BioLegend	108126 (1:100) RRID: AB_10645327
Rat anti-mouse CD150-AF488 (TC15-12F12.2)	BioLegend	115916 (1:50) RRID: AB_528744
Rat anti-mouse CD150-PE (TC15-12F12.2)	BioLegend	115904 (1:100) RRID: AB_313683
Streptavidin-PB	Thermo Fisher Scientific	S11222 (1:100)
Armenian hamster anti-mouse CD48-AF700 (HM48-1)	BioLegend	103426 (1:100) RRID: AB_10612755
Rat anti-mouse CD135-PE-Cy5 (A2F10)	BioLegend	135312 (1:100) RRID: AB_2263031
Armenian hamster anti-mouse CD34-APC (HM34)	BioLegend	128612 (1:50) RRID: AB_10553896
PE anti-mouse CD121a (IL-1 R, Type I/p80) Antibody (JAMA-147)	BioLegend	113505 (1:50) RRID: AB_2125036
IL-1 alpha Monoclonal Antibody-PE (ALF-161)	eBioscience	12-7011-82 (1:50) RRID: AB_466144
Armenian Hamster IgG Isotype Control-PE (eBio299Arm)	eBioscience	12-4888-81 (1:50) RRID: AB_470073
Goat purified anti-mouse c-kit	Fluidigm	3173004B (1:500) RRID: AB_2811230
Rat purified anti-mouse Gr-1	Fluidigm	3141005B (1:500) RRID: AB_10013483
Rabbit anti-DsRed	Takara Bio USA, Inc.	632496 (1:250) RRID: AB_2313568
Donkey anti-Rabbit IgG (H+L) conjugated with Cy-3	Jackson ImmunoResearch	711-166-152 (1:250) RRID: AB_2313568
Goat anti-Armenian hamster IgG (H+L) conjugated with AF488	Jackson ImmunoResearch	127-545-160 (1:250) RRID: AB_2338997
Donkey anti-Rat IgG (H+L) conjugated with AF647	Jackson ImmunoResearch	712-606-153 (1:250) RRID: AB_2340696
PerCP anti-mouse CD45 Antibody	Biolegend	103130 (1:100) RRID: AB_893339
Pacific Blue™ anti-mouse CD41 Antibody	Biolegend	133931 (1:100) RRID: AB_2750525
Brilliant Violet 785 anti-mouse Ly-6G	Biolegend	127645 (1:100) RRID: AB_2566317
BV605 anti-mouse I-A/I-E antibody	Biolegend	107639 (1:100) RRID: AB_2565894
Biotin anti-mouse CD19	Biolegend	115503 (1:100) RRID: AB_313683
Anti-mouse XCR1 BV650 (ZET)	Biolegend	148220 (1:100) RRID: AB_313638
CD170 (Siglec F) Monoclonal Antibody (1RNM44N), PerCP-eFluor™ 710	eBioscience	46-1702-80 (1:100) RRID: AB_2573724
APC anti-mouse CD172a (SIRPα) Antibody	Biolegend	144013 (1:100) RRID: AB_2564060

Reagents and Tools table (continued)

Reagent/Resource	Reference or Source	Identifier or Catalog Number
<b>Chemicals, enzymes and other reagents</b>		
Arakinra	KINERET	
Pam3csk4	InvivoGen	tlrl-pms
LPS-EB Ultrapure	InvivoGen	tlrl-3pelps
Mouse G-CSF ELISA Kit	Proteintech	KE10025
LEGENDplex™ Mouse HSC Panel (13-plex) with Filter Plate	Bio Legend	740676
LEGENDplex™ Mouse inflammation Panel (13-plex) with Filter Plate	Bio Legend	740150
Clodronate Liposomes & Control Liposomes (PBS)	Liposoma	CP-005-005
<b>Software</b>		
FlowJo	BD Life Sciences	<a href="#">RRID: SCR_008520</a>
Imaris	Oxford Instruments	<a href="#">RRID: SCR_007370</a>
IBM SPSS Statistics V22.0 and V26.0	IBM	<a href="#">RRID: SCR_019096</a>
GraphPad Prism v9	GraphPad Softwar	<a href="#">RRID: SCR_002798</a>
Adobe Illustrator 2023 (v27.1.1)	Adobe	<a href="#">RRID: SCR_010279</a>
LEGENDPlex Software v8.0	BioLegend	software provied by BioLegend as part of the LegendPlex kit for cytokine analysis
<b>Other</b>		
Leica Cryostat CM1950	Leica	
Leica TCS SP8 DLS	Leica	
BD Cell sorter Aria IIIu	BD Biosciences	
BD Cell analyzer Canto II	BD Biosciences	
BD Cell analyzer Symphony	BD Biosciences	
BD LSR Fortessa	BD Biosciences	

## Methods and Protocols

### Mice

C57BL/6, B6.SJL, *Hlf<sup>tdTomato+</sup>* reporter (Yokomizo *et al*, 2019), BALB/c, MSTRG (Rongvaux *et al*, 2014), *Myd88;Trif<sup>-/-</sup>* and *TLR2;4<sup>-/-</sup>* mice were maintained at the Center for Animal Resources and Development at Kumamoto University. *IL-1 $\alpha$ <sup>-/-</sup>* mice were maintained at the Institute of Medical Science, The University of Tokyo. CD45.1/2<sup>+</sup> mice were bred by crossing C57BL/6 (CD45.2<sup>+</sup>) with B6.SJL (CD45.1<sup>+</sup>). *Hlf<sup>tdTomato+</sup>* reporter mice (CD45.1<sup>+</sup>) were kindly provided by Dr. Tomomasa Yokomizo (Kumamoto University; Yokomizo *et al*, 2019). *Myd88; Trif<sup>-/-</sup>* and *Tlr2;4<sup>-/-</sup>* mice (CD45.2<sup>+</sup>) were purchased from Oriental BioService (Kyoto, Japan). All the experiments were done with 6–14 weeks-old mice. Experiments were approved by the Animal Care and Use Committee of Kumamoto University (A2021-034).

### Preparation of live bacteria and bacterial components

For colony forming (CFU) assay, glycerol stocks of *A. muciniphila* were thawed and precultured in the GAM medium (Nissui Pharmaceutical) overnight under anaerobic conditions before plated on the GAM agarose plate. The number of colonies on the plate was counted after 3 days culture under anaerobic conditions and calculated back to the concentration of the original bacterial suspension

seeded on the plate. In the preliminary experiment, the concentration of bacterial suspension whose optical density at 600 nm (OD<sub>600</sub>) was 1.0 was  $7.0 \times 10^8$  CFU/ml. Based on this, the concentration of  $1.0 \times 10^7$ ,  $1.0 \times 10^8$ , or  $1.0 \times 10^9$  CFU/200  $\mu$ l was estimated and prepared in anaerobic PBS for the live *A. m.* injection into mice. The actual concentration of the bacterial suspension was confirmed by CFU assay using the same aliquot of bacterial suspension. For the preparation of microbial membrane fraction, *A. muciniphila* or *Bacteroides thetaiotaomicron* was cultured in GAM medium under anaerobic conditions for 2 to 3 days, were centrifuged at 15,000 *g* for 5 min at 4°C and bacterial pellet was washed and resuspended in PBS. Bacterial suspension was then sonicated using a sonicator (Smurt, Microtec, Funabashi, Japan) with 30 s intervals on ice at least 20 times. After sonication efficiency was confirmed by gram-staining, bacterial suspension was ultracentrifuged at 100,000 *g* for 60 min at 4°C (Optima XE-90, Beckman Coulter, Brea, CA) and pellet was resuspended in PBS. Protein concentration of bacterial membrane fraction suspension was determined by Bio-Rad protein assay (#5000006, BioRad, Hercules, CA).

### Organ weight and blood count

Liver and spleen were isolated from treated mice and weighed. Peripheral blood was obtained from orbital vein using heparin-coated capillaries (HIRSCHMANN, Eberstadt, Germany).



Hematological parameters were assessed using the hematology analyzer (Celltac  $\alpha$  MEK-6358, Nihon Kohden, Tokyo, Japan).

#### TLR agonist and IL-1Ra treatment, and macrophage deletion

For the TLR agonist treatment, mice were *i.p.* injected with the following reagents: 200  $\mu$ g of LPS, corresponding to 200EU LPS-EB Ultrapure (#14954-81, Invivogen, San Diego, CA), 200  $\mu$ g of Pam3CSK4 (#14954-61, Invivogen), 200  $\mu$ g of *A. m.* or PBS as vehicle control. Membrane fraction suspension. For the IL-1R inhibition experiment, mice were daily *i.p.* injected with 37  $\mu$ g of Anakinra (Kineret, IL-1ra, Swedish Orphan Biovitrum AB, Stockholm, Sweden) over 2 weeks until the mice were sacrificed for analysis. *A. m.* was injected once 1 day after the first Anakinra injection in this experiment. For macrophage deletion assay, 3 days before *A. m.* injection, mice were *i.p.* injected with 200  $\mu$ l/20 mg of either clodronate liposome or control liposome (liposma, Tokyo Future Style, Inc.) over twice a week until the mice were sacrificed for analysis. *A. m.* was injected at 3 days after the first liposome injection.

#### FACS analysis

BM and spleen were harvested from treated mice and incubated with the following biotinylated antibodies against the lineage (Lin) markers: B220 (RA3-6B2), CD3 $\epsilon$  (145-2C11), CD4 (GK1.5), CD8 $\alpha$  (53-6.7), NK1.1 (PK136), CD11b (M1/70), Ter119 (Ter119), and Gr-1 (RB6-8C5) together with the following fluorescence-conjugated antibodies: c-Kit (2B8), Sca-1 (D7), CD34 (HM34), Flt3 (A2F10), CD150 (TC15-12F12.2), CD48 (HM48-1), CD16/32 (93), IL-7R $\alpha$  (A7R34) and CD86 (GL-1); for the mature cell analysis, anti-CD16/CD32 antibody was used to block Fc $\gamma$  receptors before fluorescent antibodies staining. B220 (RA3-6B2), CD3 $\epsilon$  (145-2C11), F4/80 (BM8), Ly6G (1A8), Ly6C (HK1.4) and CD11b (M1/70). For myeloid specific staining, samples were incubated with the following biotinylated antibodies against the lineage (Lin) markers: CD3 $\epsilon$ , CD4, CD8 $\alpha$ , NK1.1, Ter119, then stained with the following fluorescence-conjugated antibodies: CD45 (30-F11), F4/80, MHC II (M5/114.15.2), XCR1 (ZET), Ly6G, B220, Siglec F (1RNM44N), CD11c, CD172a (P84), Ly6C, CD11b. For lymphoid cell staining, samples were incubated with the following fluorescence-conjugated antibodies: CD45, CD19 (6D5), CD3 $\epsilon$ , CD41 (MWRreg30), CD11b. For intracellular cytokine staining, cells stained with surface marker antibodies were incubated in fixation/permeabilization buffer (eBiosciences) for 30 min at room temperature, followed by staining with either anti-IL-1 $\alpha$ -PE (Invitrogen) or isotype control antibodies for 30 min at 4°C. Stained cells were analyzed on FACS Canto II, Aria III, Symphony or LSR Fortessa (BD Biosciences, Franklin Lakes, NJ). Data were analyzed using FlowJo (BD Biosciences).

#### Competitive repopulation assay

$3 \times 10^5$  whole BM (WBM) cells and  $1 \times 10^6$  whole splenocytes were isolated from either *A. m.*- or PBS-treated WT mice (CD45.1<sup>+</sup>) at 14 days post injection and transplanted intravenously into lethally irradiated (10Gy), 8–10 weeks old WT mice (CD45.2<sup>+</sup>) together with  $3 \times 10^5$  WBM competitor cells isolated from WT mice (CD45.1/CD45.2) via tail vein within 24 h. PB donor chimerism was assessed every 4 weeks, up to 16 weeks and in BM up to 20 weeks post transplantation. Mice were sacrificed 20 weeks after transplantation and donor chimerism was assessed in the BM. For HSC

transplantation, 50 LSK CD48<sup>-</sup>CD150<sup>+</sup> cells were sorted into each well of a 96-well plate from splenocytes at 14 days post injection, and co-transplanted with  $2 \times 10^5$  F1 competitor cells into lethally irradiated recipient, followed by monthly PB donor chimerism assessment for up to 12 weeks.

#### Measurement of inflammatory or HSC-related factors

Cell lysates were obtained by adding 100  $\mu$ l of 500  $\mu$ M 1 $\times$  RIPA buffer (Abcam, Cambridge, UK) to  $1 \times 10^7$  splenocytes or BM cells. For serum isolation, PB was obtained via orbital vein using glass capillaries without anti-coagulant and left at room temperature for 20 min followed by centrifugation at 1,000 g for 15 min. To obtain BM fluid, two tibiae were flushed out with 0.5 ml BSA/PBS (0.1%), followed by centrifugation at 1,100 g for 5 min at 4°C. For spleen fluid, a small piece of the spleen (5 mg) was mashed with 0.1 ml BSA/PBS (0.1%) between a pair of glass slides, followed by centrifugation at 1,100 g for 5 min at 4°C. Samples were all stored at  $-80^\circ\text{C}$  for cytokine measurement after collection. G-CSF was quantified by Mouse G-CSF ELISA Kit (#KE10025, Proteintech, Rosemont, IL) according to the manufacturer's instructions. Other cytokines were measured by Legendplex<sup>TM</sup> Mouse Inflammation Panel (#740150, BioLegend) and Legendplex<sup>TM</sup> Mouse HSC Panel (#740150, BioLegend) according to the manufacturer's instructions.

#### Spleen imaging

Spleen samples harvested from *Hlf<sup>tdTomato+</sup>* reporter mice at 14 days post *A. m.* lysate injection were fixed in 4% PFA at 4°C overnight, washed in PBS for 30 min and cryoprotected with 30% sucrose in PBS at 4°C overnight. Samples were embedded in O.C.T compound (Sakura Finetek Japan, Tokyo, Japan) and frozen, followed by sectioning (20  $\mu$ m) using a Leica CM1950 cryostat (Leica Biosystems, Wezlar, Germany). Sectioned samples were washed with PBS three times to remove excess O.C.T compound and incubated with the following primary antibodies at 4°C overnight: RFP (PM005, MBL), c-Kit (AF1356, R&D systems, Minneapolis, MN), Gr-1 (RB6-8C5, 16-5931-81, Thermo Fisher Scientific). Samples were washed with PBS three times and stained with the following secondary antibodies at 37°C for 1 h: Donkey anti-Rabbit IgG (H + L) conjugated with Cy-3 and donkey anti-Rat IgG (H + L) conjugated with Alexa Fluor 647 (Jackson ImmunoResearch, West Grove, PA). F4/80-PE (BM8, Thermo Fisher Scientific), Ly6G-AF647 (1A8, BioLegend) were used as directly fluorescent conjugated antibodies for immunofluorescent staining. Images were obtained with a Leica CS SP8 DLS confocal microscope (Leica Biosystems). Three-dimensional (3D) reconstructions were generated from z-stack images using the microscopy imaging analysis software Imaris (Bitplane, Zurich, Switzerland).

#### Quantification and statistical analysis

Statistical analysis was performed using SPSS version 22.0 and 26.0, and GraphPad prism 9.3.1. Two-group comparisons were analyzed with the Student's *t*-test (two-tailed *t*-test). Multigroup comparisons were performed by a one-way analysis of variance (ANOVA) followed by the Tukey–Kramer multiple comparisons test if variances were equal, and Dunnett's *C* test if variances were not equal. For time course kinetics, Two-way ANOVA with Šidák's multiple comparisons test were performed. All results are expressed as means  $\pm$  standard error of the mean (SEM). The criterion of significance was set at  $P < 0.05$ .

## Data availability

This study includes no data deposited in external repositories.

**Expanded View** for this article is available [online](#).

## Acknowledgements

We would like to thank the International Core-facility of Advanced Life Science at Kumamoto University for their logistical and technical assistance and the Center for Animal Resources and Development at Kumamoto University for mice maintenance. We also thank Dr. Sayuri Nakata and Dr. Ayane Takao for her technical assistance. This work was supported by China Scholarship Council (201908440506 to YW), JST ERATO (JPMJER1902 to SF), AMED-CREST (JP21gm1010009 to SF), the Food Science Institute Foundation (to SF), KAKENHI from JSPS (15H01519 and 17H05651 to HT), KAKETSUKEN (The Chemo-Sero-Therapeutic Research Institute) (to TM, MS and HT), JST FOREST (JPMJFR2000 to HT), the Uehara Memorial Foundation (to HT), Princess Takamatsu Cancer Research Fund (to HT), Takeshi Nagao Intractable Diseases Research Fund (to HT), The NOVARTIS Foundation (to HT), The Tokyo Biochemical Research Foundation (to HT), and the Center for Metabolic Regulation of Healthy Aging at Kumamoto University (to HT).

## Author contributions

**Yuxin Wang:** Data curation; software; validation; investigation; writing – original draft; writing – review and editing. **Tatsuya Morishima:** Conceptualization; formal analysis; investigation. **Maiko Sezaki:** Data curation; software. **Ryo Sato:** Data curation. **Gaku Nakato:** Resources; methodology. **Shinji Fukuda:** Conceptualization; resources; funding acquisition; methodology. **Kouji Kobiyama:** Investigation; methodology. **Ken J Ishii:** Investigation; methodology. **Yuhua Li:** Supervision. **Hitoshi Takizawa:** Conceptualization; supervision; funding acquisition; writing – original draft; project administration; writing – review and editing.

## Disclosure and competing interests statement

The authors declare that they have no conflict of interest.

## References

- Akashi K, Traver D, Miyamoto T, Weissman IL (2000) A clonogenic common myeloid progenitor that gives rise to all myeloid lineages. *Nature* 404: 193–197
- Akira S, Takeda K (2004) Toll-like receptor signalling. *Nat Rev Immunol* 4: 499–511
- Ansaldi E, Slayden LC, Ching KL, Koch MA, Wolf NK, Plichta DR, Brown EM, Graham DB, Xavier RJ, Moon JJ *et al* (2019) *Akkermansia muciniphila* induces intestinal adaptive immune responses during homeostasis. *Science* 364: 1179–1184
- Bae M, Cassilly CD, Liu X, Park S-M, Tusi BK, Chen X, Kwon J, Filipčík P, Bolze AS, Liu Z *et al* (2022) *Akkermansia muciniphila* phospholipid induces homeostatic immune responses. *Nature* 608: 168–173
- Balmer ML, Schurch CM, Saito Y, Geuking MB, Li H, Cuenca M, Kovtonyuk LV, McCoy KD, Hapfelmeier S, Ochsenbein AF *et al* (2014) Microbiota-derived compounds drive steady-state granulopoiesis via MyD88/TICAM signaling. *J Immunol* 193: 5273–5283
- Biragyn A, Ferrucci L (2018) Gut dysbiosis: a potential link between increased cancer risk in ageing and inflammaging. *Lancet Oncol* 19: e295–e304
- Burberry A, Zeng MY, Ding L, Wicks I, Inohara N, Morrison SJ, Nunez G (2014) Infection mobilizes hematopoietic stem cells through cooperative NOD-like receptor and Toll-like receptor signaling. *Cell Host Microbe* 15: 779–791
- Cendrowski J, Maminska A, Miaczynska M (2016) Endocytic regulation of cytokine receptor signaling. *Cytokine Growth Factor Rev* 32: 63–73
- Chan J, Atianand M, Jiang Z, Carpenter S, Aiello D, Elling R, Fitzgerald KA, Caffrey DR (2015) Cutting edge: a natural antisense transcript, AS-IL1alpha, controls inducible transcription of the proinflammatory cytokine IL-1alpha. *J Immunol* 195: 1359–1363
- Curtis BM, Widmer MB, deRoos P, Qvarnstrom EE (1990) IL-1 and its receptor are translocated to the nucleus. *J Immunol* 144: 1295–1303
- Derosa L, Routy B, Thomas AM, Iebba V, Zalzman G, Friard S, Mazieres J, Audigier-Valette C, Moro-Sibilot D, Goldwasser F *et al* (2022) Intestinal *Akkermansia muciniphila* predicts clinical response to PD-1 blockade in patients with advanced non-small-cell lung cancer. *Nat Med* 28: 315–324
- Derrien M, Vaughan EE, Plugge CM, de Vos WM (2004) *Akkermansia muciniphila* gen. nov., sp. nov., a human intestinal mucin-degrading bacterium. *Int J Syst Evol Microbiol* 54: 1469–1476
- Derrien M, Collado MC, Ben-Amor K, Salminen S, de Vos WM (2008) The Mucin degrader *Akkermansia muciniphila* is an abundant resident of the human intestinal tract. *Appl Environ Microbiol* 74: 1646–1648
- Di Paolo NC, Shayakhmetov DM (2016) Interleukin 1alpha and the inflammatory process. *Nat Immunol* 17: 906–913
- Djalalietti M, Bessler H, Rifkind RA (1972) Hematopoiesis in the embryonic mouse spleen: an electron microscopic study. *Blood* 39: 826–841
- Esplin BL, Shimazu T, Welner RS, Garrett KP, Nie L, Zhang Q, Humphrey MB, Yang Q, Borghesi LA, Kincaid PW (2011) Chronic exposure to a TLR ligand injures hematopoietic stem cells. *J Immunol* 186: 5367–5375
- Essers MA, Offner S, Blanco-Bose WE, Waibler Z, Kalinke U, Duchosal MA, Trumpp A (2009) IFNalpha activates dormant haematopoietic stem cells in vivo. *Nature* 458: 904–908
- Fibbe WE, Hamilton MS, Laterveer LL, Kibbelaar RE, Falkenburg JH, Visser JW, Willemze R (1992) Sustained engraftment of mice transplanted with IL-1-primed blood-derived stem cells. *J Immunol* 148: 417–421
- Firestein GS (2003) Evolving concepts of rheumatoid arthritis. *Nature* 423: 356–361
- Ganesh BP, Klopffleisch R, Loh G, Blaut M (2013) Commensal *Akkermansia muciniphila* exacerbates gut inflammation in Salmonella Typhimurium-infected gnotobiotic mice. *PLoS ONE* 8: e74963
- Golub R, Tan J, Watanabe T, Brendolan A (2018) Origin and immunological functions of spleen stromal cells. *Trends Immunol* 39: 503–514
- Gracey E, Vereecke L, McGovern D, Frohling M, Schett G, Danese S, De Vos M, Van den Bosch F, Elewaut D (2020) Revisiting the gut-joint axis: links between gut inflammation and spondyloarthritis. *Nat Rev Rheumatol* 16: 415–433
- Griseri T, McKenzie BS, Schiering C, Powrie F (2012) Dysregulated hematopoietic stem and progenitor cell activity promotes interleukin-23-driven chronic intestinal inflammation. *Immunity* 37: 1116–1129
- Hernandez G, Mills TS, Rabe JL, Chavez JS, Kuldaneck S, Kirkpatrick G, Noetzli L, Jubair WK, Zanche M, Myers JR *et al* (2020) Pro-inflammatory cytokine blockade attenuates myeloid expansion in a murine model of rheumatoid arthritis. *Haematologica* 105: 585–597
- Horai R, Asano M, Sudo K, Kanuka H, Suzuki M, Nishihara M, Takahashi M, Iwakura Y (1998) Production of mice deficient in genes for interleukin (IL)-1α, IL-1β, IL-1α/β, and IL-1 receptor antagonist shows that IL-1β is crucial in turpentine-induced fever development and glucocorticoid secretion. *J Exp Med* 187: 1463–1475
- Inra CN, Zhou BO, Acar M, Murphy MM, Richardson J, Zhao Z, Morrison SJ (2015) A perisinusoidal niche for extramedullary haematopoiesis in the spleen. *Nature* 527: 466–471

- Kanayama M, Izumi Y, Yamauchi Y, Kuroda S, Shin T, Ishikawa S, Sato T, Kajita M, Ohteki T (2020) CD86-based analysis enables observation of bona fide hematopoietic responses. *Blood* 136: 1144–1154
- Khosravi A, Yanez A, Price JG, Chow A, Merad M, Goodridge HS, Mazmanian SK (2014) Gut microbiota promote hematopoiesis to control bacterial infection. *Cell Host Microbe* 15: 374–381
- Kovtonyuk LV, Caiado F, Garcia-Martin S, Manz EM, Helbling PM, Takizawa H, Boettcher S, Al-Shahrour F, Nombela-Arrieta C, Slack E et al (2021) IL-1 mediates microbiome-induced inflamm-ageing of hematopoietic stem cells in mice. *Blood* 139: 44–58
- Krishnan S, Wemyss K, Prise IE, McClure FA, O'Boyle C, Bridgeman HM, Shaw TN, Grainger JR, Konkel JE (2021) Hematopoietic stem and progenitor cells are present in healthy gingiva tissue. *J Exp Med* 218: e20200737
- Lee S, Kim H, You G, Kim YM, Lee S, Le VH, Kwon O, Im SH, Kim YM, Kim KS et al (2019) Bone marrow CX3CR1+ mononuclear cells relay a systemic microbiota signal to control hematopoietic progenitors in mice. *Blood* 134: 1312–1322
- Li J, Lee DS, Madrenas J (2013) Evolving bacterial envelopes and plasticity of TLR2-dependent responses: basic research and translational opportunities. *Front Immunol* 4: 347
- Lin Z, Shi JL, Chen M, Zheng ZM, Li MQ, Shao J (2022) CCL2: an important cytokine in normal and pathological pregnancies: a review. *Front Immunol* 13: 1053457
- Liu Y, Yang M, Tang L, Wang F, Huang S, Liu S, Lei Y, Wang S, Xie Z, Wang W et al (2022) TLR4 regulates RORgammat(+) regulatory T-cell responses and susceptibility to colon inflammation through interaction with *Akkermansia muciniphila*. *Microbiome* 10: 98
- Lukens JR, Vogel P, Johnson GR, Kelliher MA, Iwakura Y, Lamkanfi M, Kanneganti TD (2013) RIP1-driven autoinflammation targets IL-1 $\alpha$  independently of inflammasomes and RIP3. *Nature* 498: 224–227
- MacNamara KC, Jones M, Martin O, Winslow GM (2011) Transient activation of hematopoietic stem and progenitor cells by IFN $\gamma$  during acute bacterial infection. *PLoS ONE* 6: e28669
- Massberg S, Schaerli P, Knezevic-Maramica I, Kollnberger M, Tubo N, Moseman EA, Huff IV, Junt T, Wagers AJ, Mazo IB et al (2007) Immunosurveillance by hematopoietic progenitor cells trafficking through blood, lymph, and peripheral tissues. *Cell* 131: 994–1008
- Mayer-Barber KD, Andrade BB, Barber DL, Hieny S, Feng CG, Caspar P, Oland S, Gordon S, Sher A (2011) Innate and adaptive interferons suppress IL-1 $\alpha$  and IL-1 $\beta$  production by distinct pulmonary myeloid subsets during *Mycobacterium tuberculosis* infection. *Immunity* 35: 1023–1034
- Mebius RE, Kraal G (2005) Structure and function of the spleen. *Nat Rev Immunol* 5: 606–616
- Migliorini P, Italiani P, Pratesi F, Puxeddu I, Boraschi D (2020) The IL-1 family cytokines and receptors in autoimmune diseases. *Autoimmun Rev* 19: 102617
- Morita Y, Iseki A, Okamura S, Suzuki S, Nakauchi H, Ema H (2011) Functional characterization of hematopoietic stem cells in the spleen. *Exp Hematol* 39: 351–359
- Nakamura-Ishizu A, Takubo K, Kobayashi H, Suzuki-Inoue K, Suda T (2015) CLEC-2 in megakaryocytes is critical for maintenance of hematopoietic stem cells in the bone marrow. *J Exp Med* 212: 2133–2146
- Neta R, Sztein MB, Oppenheim JJ, Gillis S, Douches SD (1987) The in vivo effects of interleukin 1. I. Bone marrow cells are induced to cycle after administration of interleukin 1. *J Immunol* 139: 1861–1866
- Newman KA, Akhtari M (2011) Management of autoimmune neutropenia in Felty's syndrome and systemic lupus erythematosus. *Autoimmun Rev* 10: 432–437
- Papadaki HA, Kritikos HD, Valatas V, Boumpas DT, Eliopoulos GD (2002a) Anemia of chronic disease in rheumatoid arthritis is associated with increased apoptosis of bone marrow erythroid cells: improvement following anti-tumor necrosis factor- $\alpha$  antibody therapy. *Blood* 100: 474–482
- Papadaki HA, Marsh JC, Eliopoulos GD (2002b) Bone marrow stem cells and stromal cells in autoimmune cytopenias. *Leuk Lymphoma* 43: 753–760
- Pietras EM, Mirantes-Barbeito C, Fong S, Loeffler D, Kovtonyuk LV, Zhang S, Lakshminarasimhan R, Chin CP, Techner JM, Will B et al (2016) Chronic interleukin-1 exposure drives haematopoietic stem cells towards precocious myeloid differentiation at the expense of self-renewal. *Nat Cell Biol* 18: 607–618
- Plovier H, Everard A, Druart C, Depommier C, Van Hul M, Geurts L, Chilloux J, Ottman N, Duparc T, Lichtenstein L et al (2017) A purified membrane protein from *Akkermansia muciniphila* or the pasteurized bacterium improves metabolism in obese and diabetic mice. *Nat Med* 23: 107–113
- Rogler G, Singh A, Kavanaugh A, Rubin DT (2021) Extraintestinal manifestations of inflammatory bowel disease: current concepts, treatment, and implications for disease management. *Gastroenterology* 161: 1118–1132
- Rongvaux A, Willinger T, Martinek J, Strowig T, Gearty SV, Teichmann LL, Saito Y, Marches F, Halene S, Palucka AK et al (2014) Development and function of human innate immune cells in a humanized mouse model. *Nat Biotechnol* 32: 364–372
- Routy B, Le Chatelier E, Derosa L, Duong CPM, Alou MT, Daillere R, Fluckiger A, Messaoudene M, Rauber C, Roberti MP et al (2018) Gut microbiome influences efficacy of PD-1-based immunotherapy against epithelial tumors. *Science* 359: 91–97
- Ruff WE, Greiling TM, Kriegl MA (2020) Host-microbiota interactions in immune-mediated diseases. *Nat Rev Microbiol* 18: 521–538
- Saito Y, Ellegast JM, Rafiei A, Song Y, Kull D, Heikenwalder M, Rongvaux A, Halene S, Flavell RA, Manz MG (2016) Peripheral blood CD34(+) cells efficiently engraft human cytokine knock-in mice. *Blood* 128: 1829–1833
- Sender R, Fuchs S, Milo R (2016) Revised estimates for the number of human and bacteria cells in the body. *PLoS Biol* 14: e1002533
- Sezaki M, Hayashi Y, Wang Y, Johansson A, Umemoto T, Takizawa H (2020) Immuno-modulation of hematopoietic stem and progenitor cells in inflammation. *Front Immunol* 11: 585367
- Sezaki M, Hayashi Y, Nakato G, Wang Y, Nakata S, Biswas S, Morishima T, Fakruddin M, Moon J, Ahn S et al (2022) Hematopoietic stem and progenitor cells integrate microbial signals to promote post-inflammation gut tissue repair. *EMBO J* 41: e110712
- Shono Y, Docampo MD, Peled JU, Perobelli SM, Velardi E, Tsai JJ, Slingerland AE, Smith OM, Young LF, Gupta J et al (2016) Increased GVHD-related mortality with broad-spectrum antibiotic use after allogeneic hematopoietic stem cell transplantation in human patients and mice. *Sci Transl Med* 8: 339ra371
- Sims JE, Smith DE (2010) The IL-1 family: regulators of immunity. *Nat Rev Immunol* 10: 89–102
- Takizawa H, Fritsch K, Kovtonyuk LV, Saito Y, Yakkala C, Jacobs K, Ahuja AK, Lopes M, Hausmann A, Hardt WD et al (2017) Pathogen-induced TLR4-TRIF innate immune signaling in hematopoietic stem cells promotes proliferation but reduces competitive fitness. *Cell Stem Cell* 21: 225–240
- Umemoto T, Matsuzaki Y, Shiratsuchi Y, Hashimoto M, Yoshimoto T, Nakamura-Ishizu A, Petrich B, Yamato M, Suda T (2017) Integrin  $\alpha$ h $\beta$ 3 enhances the suppressive effect of interferon- $\gamma$  on hematopoietic stem cells. *EMBO J* 36: 2390–2403

- Westerterp M, Gourion-Arsiquaud S, Murphy AJ, Shih A, Cremers S, Levine RL, Tall AR, Yvan-Charvet L (2012) Regulation of hematopoietic stem and progenitor cell mobilization by cholesterol efflux pathways. *Cell Stem Cell* 11: 195–206
- Wright DE, Wagers AJ, Gulati AP, Johnson FL, Weissman IL (2001) Physiological migration of hematopoietic stem and progenitor cells. *Science* 294: 1933–1936
- Wu Z, Huang S, Li T, Li N, Han D, Zhang B, Xu ZZ, Zhang S, Pang J, Wang S et al (2021) Gut microbiota from green tea polyphenol-dosed mice improves intestinal epithelial homeostasis and ameliorates experimental colitis. *Microbiome* 9: 184
- Yamashita M, Passegue E (2019) TNF-alpha coordinates hematopoietic stem cell survival and myeloid regeneration. *Cell Stem Cell* 25: e357
- Yokomizo T, Watanabe N, Umemoto T, Matsuo J, Harai R, Kihara Y, Nakamura E, Tada N, Sato T, Takaku T et al (2019) Hlf marks the developmental pathway for hematopoietic stem cells but not for erythro-myeloid progenitors. *J Exp Med* 216: 1599–1614